Revision of the genus Anasibirites Mojsisovics (Ammonoidea): An iconic and cosmopolitan taxon of the late Smithian (Early Triassic) extinction

Romain Jattiot, Hugo Bucher, Arnaud Brayard, Claude Monnet, James F. Jenks, Michael Hautmann

Revision of the genus *Anasibirites* Mojsisovics (Ammonoidea): An iconic and cosmopolitan taxon of the late Smithian (Early Triassic) extinction

Romain Jattiot[1, 2], Hugo Bucher[1], Arnaud Brayard[2], Claude Monnet[3], James F. Jenks[4], Michael Hautmann[1]

[1]Paläontologisches Institut der Universität Zürich, Karl Schmid-Strasse 4, 8006, Zürich, Switzerland; e-mail: romain.jattiot@pim.uzh.ch
[2]UMR CNRS 6282 Biogéosciences, Université de Bourgogne Franche-Comté, 6 Boulevard Gabriel, 21000, Dijon, France
[3]UMR CNRS 8198 Evo-Eco-Paleo, Université de Lille (Sciences et Technologies), UFR Sciences de la Terre (SN5), Cité Scientifique, 59655, Villeneuve d'Ascq, France
[4]1134 Johnson Ridge Lane, West Jordan, Utah, 84084, USA

Abstract: The family Prionitidae Hyatt represents a major component of ammonoid faunas during the Smithian (Early Triassic), and the genus *Anasibirites* Mojsisovics is the most emblematic taxon of this family. Its stratigraphical range is restricted to the beginning of the late Smithian (*Wasatchites distractus* Zone). The genus is also characterized by an unusual cosmopolitan distribution, thus contrasting with most earlier Smithian ammonoid distributions that were typically restricted by latitude. Because the late Smithian witnessed an extinction of the nekton (e.g. ammonoids, conodonts) whose amplitude is equal to or larger than that of the end-Permian crisis, the number of valid species that should be included in the genus *Anasibirites* becomes a highly relevant question when addressing this extinction at the highest possible taxonomic resolution. Based on a new extensive collection from Timor, the composition of the genus *Anasibirites* is herein revised with respect to its intraspecific and ontogenetic variations. Comprehensive morphological and biometric studies (*c.* 950 measured specimens) indicate that, of the *c.* 60 available species names, only two are valid, namely *A. kingianus* (Waagen) and *A. multiformis* Welter. Continuous ranges of intraspecific variation enable us to synonymize *A. nevolini* Zakharov, 1968 and *A. angulosus* (Waagen) with *A. kingianus*. The contribution of *Anasibirites* to species diversity during the late Smithian extinction is thus significantly less than previously estimated, therefore accentuating the severity of this event.

Key words: late Smithian extinction, Timor, *Anasibirites*, Taxonomy, intraspecific variation.

THE late Smithian genus *Anasibirites* Mojsisovics, 1896, which occurs abundantly worldwide, is an iconic index taxon marking the beginning of the late Smithian extinction (Fig. 1). The late Smithian is a short time interval (*c.* 100 kyr; Brühwiler *et al.* 2010) that witnessed the most severe intra-Triassic crisis for the nekton (*c.* 1.4 myr after the end-Permian mass extinction; Ovtcharova *et al.* 2006, 2015; Galfetti *et al.* 2007; Burgess *et al.* 2014). The late Smithian extinction as it affected ammonoids and conodonts was of equal or larger magnitude than that of the end-Permian crisis (Brühwiler *et al.* 2010).

A profusion (*c.* 60) of species names for *Anasibirites* exists in the literature (see e.g. Waagen 1895; Mathews 1929). This typological taxonomic richness essentially originates from two causes: (1) sufficiently large samples were not previously available; and (2) most species referred to this genus are based on minute morphological differences that would be considered as intraspecific variation in a population approach. Brayard and Bucher (2008) initiated a revision of the genus, taking intraspecific variation into account, and suggested the existence of only four valid species: *A. kingianus* (Waagen, 1895); *A. multiformis* Welter, 1922; *A. nevolini* Zakharov, 1968; and *A. pluriformis* Guex, 1978. Subsequently, Brühwiler and Bucher (2012a) re-assigned *A. pluriformis* to the genus *Truempyceras*, a distinct genus of middle Smithian age assigned to Arctoceratidae. These authors also re-instated another species of *Anasibirites*, namely *A. angulosus* (Waagen, 1895), characterized by its tabulate venter and ornamentation consisting of biconcave ribs of highly varying strength (Brühwiler and Bucher 2012a).

In summary, according to the latest studies (Brühwiler and Bucher 2012a; Brayard *et al.* 2013), four valid species of *Anasibirites* can apparently be differentiated. Some of
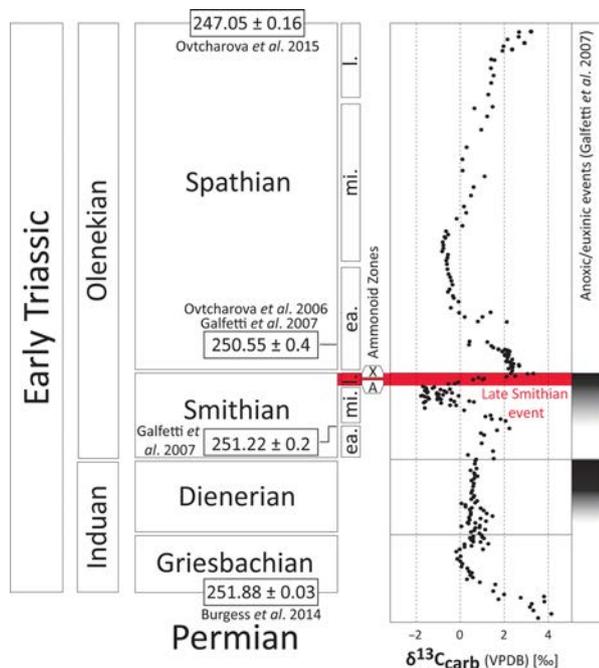
FIG. 1. Early Triassic subdivision calibrated with published radiometric ages (Ovtcharova *et al.* 2006; Galfetti *et al.* 2007; Burgess *et al.* 2014). δC^{13}$_{carb}$ curves and anoxic/euxinic events from Galfetti *et al.* (2007). A, *Anasibirites*; X, *Xenoceltites*; ea., early; mi., middle; l., late. Colour online.

(Brayard and Bucher 2008), *A. kingianus* and *A. angulosus* co-occur within the *Wasatchites distractus* beds in Pakistan (Brühwiler and Bucher 2012*a*), and *A. kingianus* and *A. multiformis* supposedly co-occur within the *Anasibirites kingianus* beds in Utah (Brayard *et al.* 2013).

According to Brayard *et al.* (2013, p. 194), different species of *Anasibirites* 'generally cannot be identified based only on their measurements and are mainly distinguished only by the strength of their ornamentation'. Kummel and Erben (1968) had earlier suggested that all previously described *Anasibirites* species should be placed in synonymy with the type species *A. kingianus*. It is also worth noting that the cosmopolitan distribution of *Anasibirites* was first recognized by Tozer (1982).

Hence, the purpose of this study was to revise the taxonomy of *Anasibirites* not only by means of classical descriptive studies, but also by means of quantitative biometric analyses, based on an extensive collection from Timor (*c.* 900 measured specimens of *Anasibirites*) and comparative material from several localities distributed worldwide (Spitsbergen, Nevada, Utah, Idaho, Guangxi, Salt Range, Spiti, Kashmir and Oman; Fig. 2).

GEOLOGICAL SETTING

Palaeogeographical context

Presently, Timor Island is located in the south-eastern part of the Indonesian archipelago, 1500 km east of Java

them co-occur within the same beds in different localities. For instance, *A. multiformis* and *A. nevolini* co-occur within the *Anasibirites multiformis* beds in Guangxi
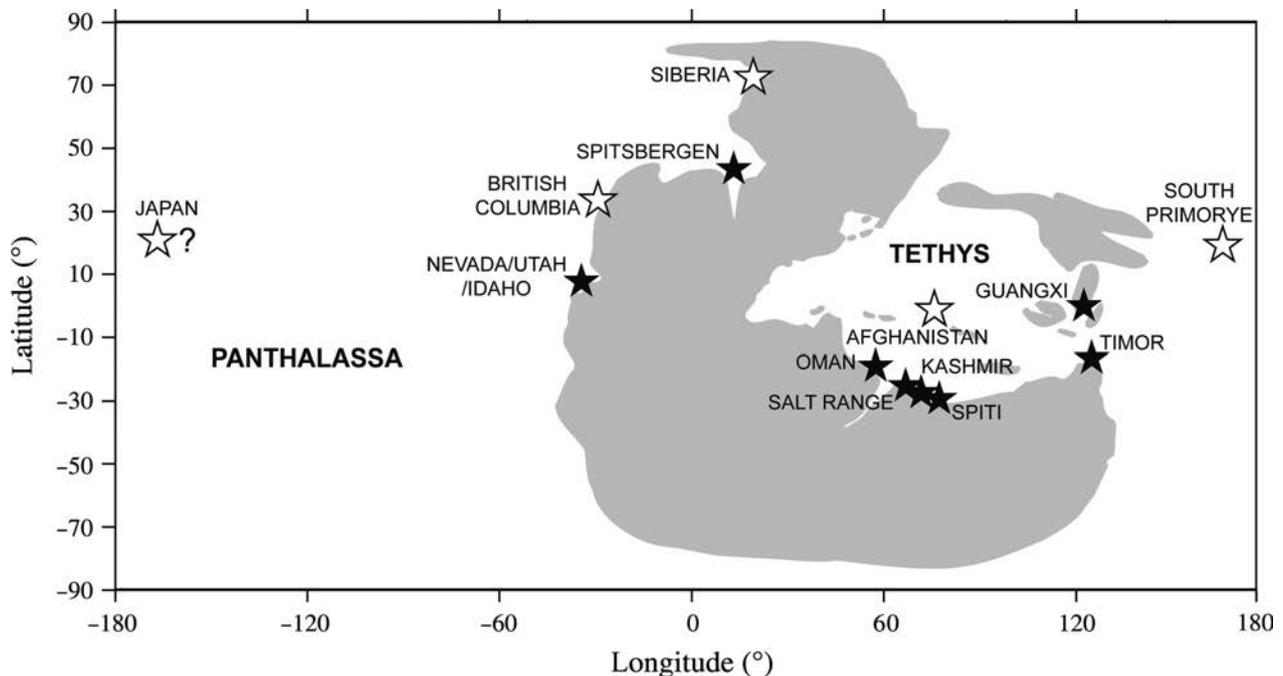
FIG. 2. Late Smithian distribution of *Anasibirites* (modified from Brayard *et al.* 2009). Black stars represent localities that yielded material for this study.

and 400 km north-west of northern Australia (Fig. 3A). During the Early Triassic, Timor was located in the eastern part of Pangea (c. −15° latitude and 125° longitude; Fig. 2) and off the northern Australian margin, in the transition zone between the Tethyan and Panthalassic realms. Ammonoids from Timor mainly come from highly fossiliferous sediments termed the 'Cephalopod Limestone Facies' (Wanner 1913). This facies occurs as exotic blocks, up to a few metres thick, embedded in the Cenozoic Bobonaro Formation (Charlton et al. 2009). These blocks consist of condensed sequences of pelagic limestone deposited on sea-mounts (Martini et al. 2000), but the range of ages represented by ammonoids indicates that most, if not all, stages of the Triassic are probably present (Charlton et al. 2009). Although embedded in a formation of Jurassic age, similar occurrences of exotic blocks of Early Triassic pelagic limestone are known from Oman (Tozer and Calon 1990, Brühwiler et al. 2012a).

Regarding Smithian-aged sediments of Timor, Welter (1922) described three subdivisions in his pioneer work, namely the *Meekoceras* limestone (early Smithian), the *Owenites* limestone (middle Smithian) and the *Anasibirites* limestone (late Smithian).

Localities and facies description

Welter (1922) studied a sample of 111 specimens of *Anasibirites* obtained from a single block of white limestone collected by the Molengraaff expedition (1910–1912) in the Anak Saban area of West Timor. The new *Anasibirites* specimens from West Timor studied in this work were extracted from 76 small-sized blocks (up to 50 cm in thickness) chiselled from a single block of white *Anasibirites* limestone near Noe Tobe (Fig. 3B). These are the only two known occurrences of the *Anasibirites* fauna in West Timor. Unlike the vast majority of other Smithian exotic blocks of reddish-pinkish micritic pelagic limestone (i.e. Hallstatt facies), the very rare occurrences of the late Smithian *Anasibirites* fauna are characterized by a very peculiar white lumachelle facies (Fig. 4). This very unusual facies of the *Anasibirites* fauna consists of densely packed shells embedded in successive generations of cements, with no or very little micritic matrix. Primary porosity between and within the shells is high, in contrast with other fossiliferous blocks of Early Triassic pelagic limestone. Decimetric tongues of mm- to cm-sized angular volcanic clasts are occasionally intercalated in this white lumachelle. The coating of shells by manganese oxide, which is commonly observed in other exotic Triassic blocks of Hallstatt limestone in Timor, is evidently absent in the white *Anasibirites* lumachelle. Hence, the depositional environment of the *Anasibirites* fauna stands in marked contrast with that of the early and middle Smithian pelagic limestone in Timor. It suggests either high energy conditions with winnowing of the sediment or a genuine absence of fine grained carbonate of neritic origin transported off shore by suspension. Absence of imbrication of the shells lends more credence to the second interpretation.

Associated macrofauna

In addition to the c. 900 *Anasibirites* measured specimens, the Noe Tobe block also yielded c. 200 specimens of *Hemiprionites*, including the species *H. typus* (Waagen, 1895), *H. butleri* (Mathews, 1929) and *H. klugi* Brayard and Bucher, 2008; and a few specimens of *Arctoprionites resseri* (Mathews, 1929) and *Wasatchites perrini* Mathews, 1929, as well. Also found in the block were very rare specimens of *Galfettites omani* Brühwiler and Bucher 2012b and *Subvishnuites posterus* Brühwiler et al., 2012b.

The only two specimens of *Galfettites* found in this *Anasibirites*-dominated assemblage represent the youngest known occurrence of this genus, which was hitherto only documented from faunas of middle Smithian age (Brayard and Bucher 2008, Brühwiler et al. 2012a, b, c).

Nevertheless, the age of both the Noe Tobe and Anak Saban blocks can be unequivocally assigned to the *Wasatchites distracus* beds, that is the oldest ammonoid zone of late Smithian age as established in expanded sections from the northern Indian margin (SM-12 in Brühwiler et al. 2010 and S-13 in Brühwiler et al. 2011). Moreover, no palaeontological condensation could be detected within the resolution of the zone level in these two Timor occurrences.

Among the associated bivalves of the Noe Tobe block, the overwhelmingly dominant and abundant species is assigned to *Crittendenia*? *australasiatica* (Krumbeck, 1924). We indicate the generic assignment as uncertain because distinction from similar *Eobuchia* requires morphological information on the right anterior auricle, which is not available. Although there are some reports of *Crittendenia* from the Griesbachian and the early Anisian (Komatsu et al. 2013), *Crittendenia* is typical of the late Smithian, where the genus has a remarkably wide geographical distribution both in the Tethys and in Panthalassa (Komatsu et al. 2013). Newell and Boyd (1995) suggested that *Crittendenia* might have lived pseudoplanktonically on floating objects including living ammonoids, which is in good agreement with its wide geographical distribution and its occasional occurrence in sediments that are indicative of oxygen-deficient bottom water. Bivalves other than *Crittendenia*? *australasiatica* are scarce in the Noe Tobe block fauna and belong to the widespread and long-ranging genera *Bakevellia*, *Leptochondria*, *Scythentolium* and *Permophorus*.
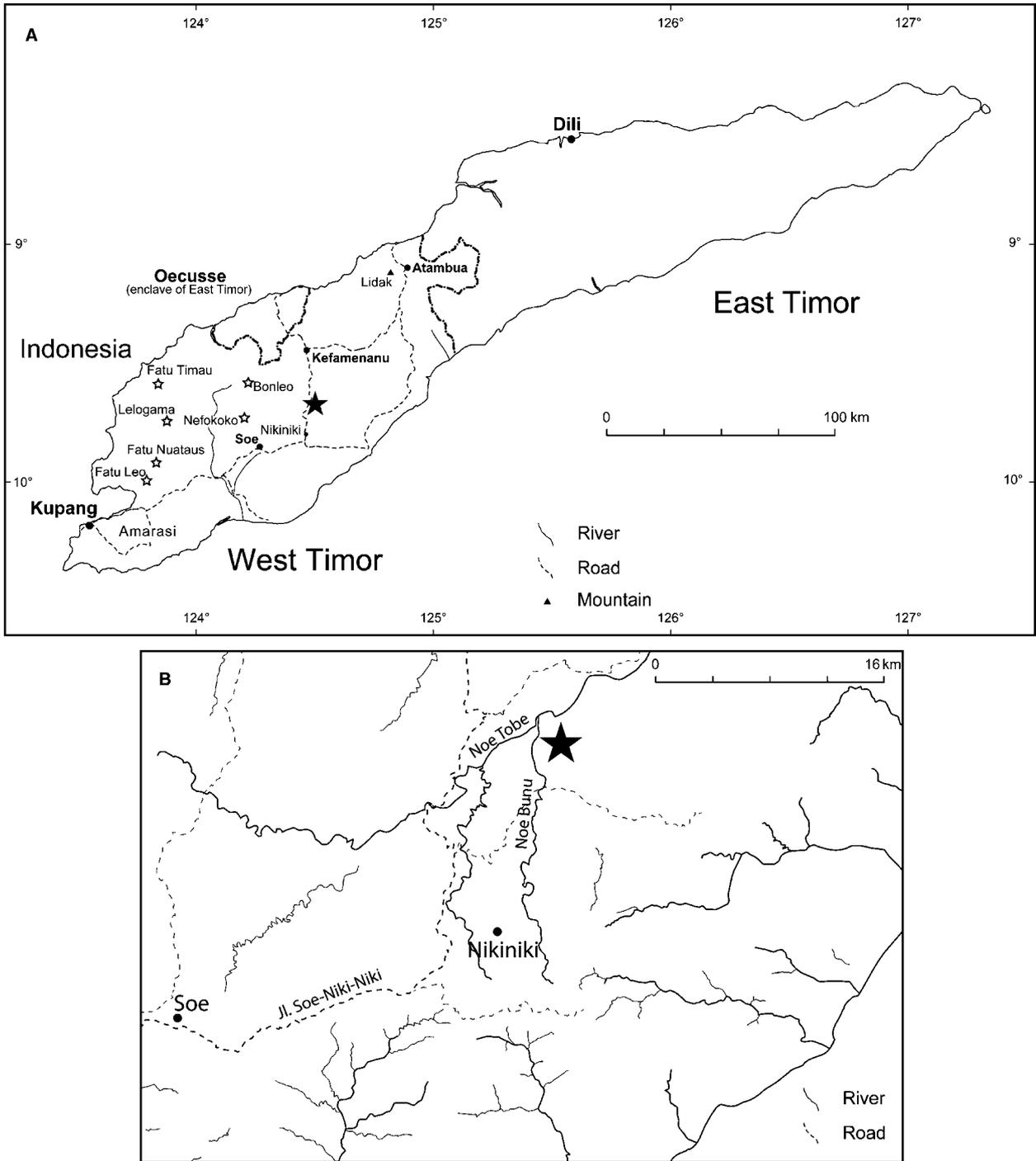
FIG. 3. A, map of Timor showing the location of Noe Tobe (black star) and other Triassic localities in West Timor (white stars; modified from Charlton *et al.* 2009). B, location of Noe Tobe (black star) at enlarged scale.

METHODS

Mode of growth of *Anasibirites*

Understanding the mode of growth of the ammonoid shell is a prerequisite to biometric, taxonomic and phy-logenetic treatments. Shells of *Anasibirites* specimens from Timor exhibit discontinuities distinct from growth lines that separate structurally independent growth segments (see Urdy *et al.* 2010). These discontinuities on the shell of *Anasibirites* specimens were frequently described as ribs in previous works. However, the
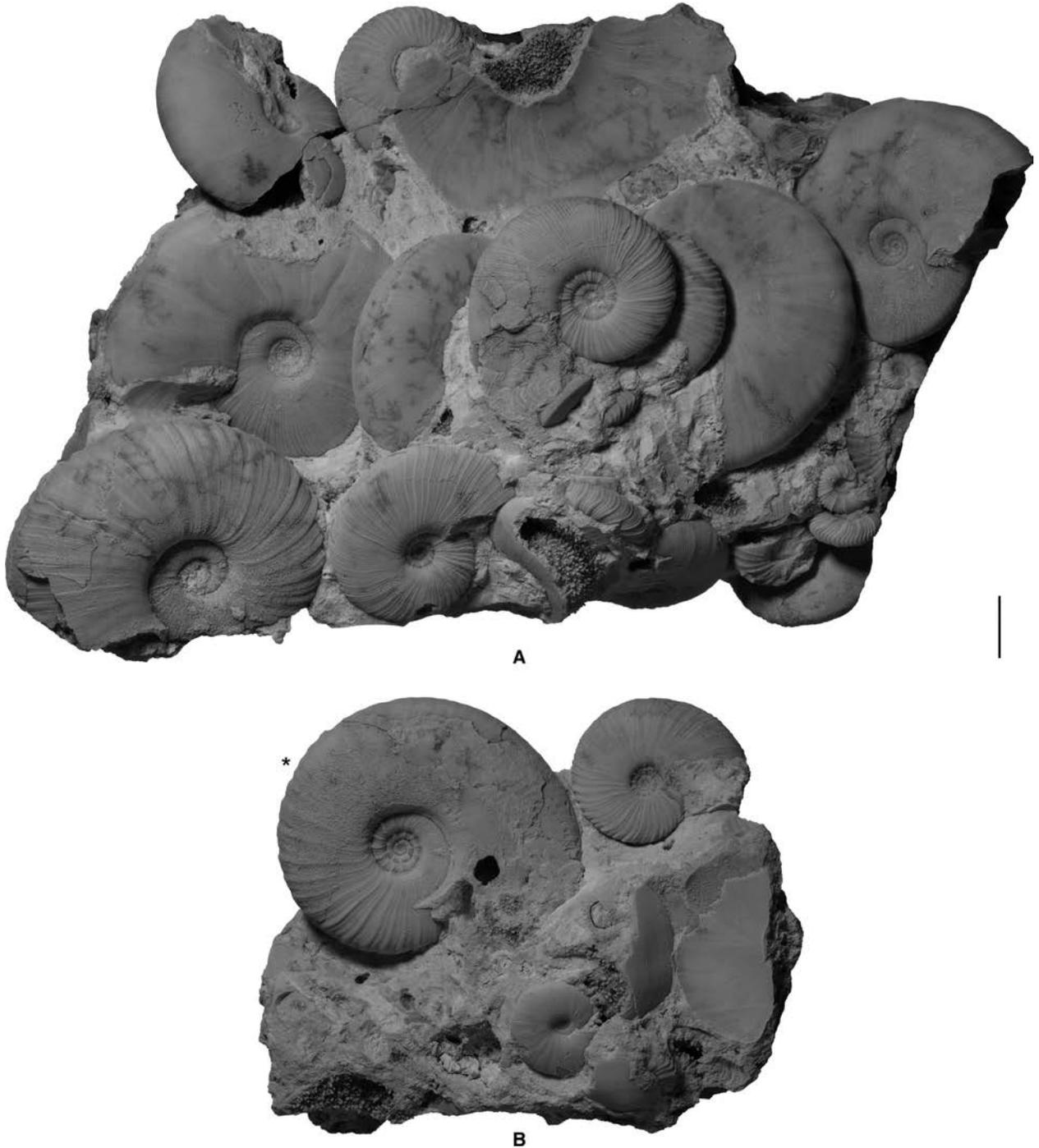
**FIG. 4.** Blocks of white lumachelle with *Anasibirites kingianus* (Waagen, 1895) from Noe Tobe (Timor). A, PIMUZ 31426. B, PIMUZ 31427. Note the absence of imbrication of shells, the exclusive presence of cement between the shells (absence of matrix), and high porosity within and between the shells. Star indicates the position of last septum. Scale bar represents 10 mm.

exceptional quality of our material from Timor allows us to assert that these discontinuities are actually megastriae (Fig. 5).

Microstructural studies of megastriae show that these are breaks in secretion (growth halts with rotation of the direction of secretion; Bucher *et al.* 1996) that generated temporary apertures (Urdy *et al.* 2010). Thus, megastriae highlight the discontinuous nature of shell secretion in that they represent intrinsic pauses in growth superimposed on the overall growth curve (Bucher *et al.* 1996).
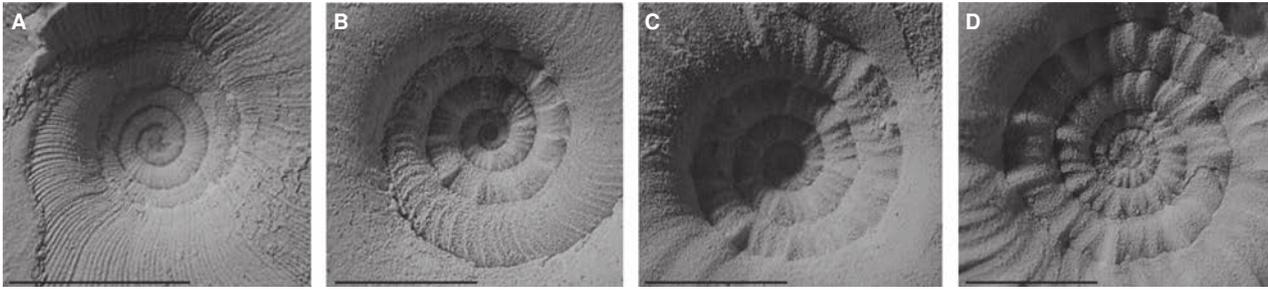
FIG. 5. Sculptural variation of early whorls in *Anasibirites multiformis* Welter, 1922 and *A. kingianus* (Waagen, 1895) from Noe Tobe (Timor). A, *A. multiformis* (PIMUZ 31394). B, *A. kingianus* (PIMUZ 31424). C, *A. kingianus* (morph *angulosus*) (PIMUZ 31476). D, *A. kingianus* (morph *nevolini*) (PIMUZ 31447). All illustrations show only megastriae, not ribs (i.e. plications). All scale bars represent 5 mm.

Megastriae are also defined as distinctive thick lines that extend continuously around the flanks and venter (Bucher and Guex 1990). They differ from lirae and ribs mainly by being asymmetrical when seen in cross-section. They also differ from lirae, growth lines and ribs by involving both the outer prismatic and nacreous layers, implying a retreat of the secreting edge of the mantle (Bucher *et al.* 1996). Furthermore, in contrast with megastriae, ribs only represent plications (corrugations) of the shell wall (Bucher *et al.* 1996). In Bucher *et al.* (1996), the term 'megastriae' was intended to represent all such features previously referred to by different terms: *alte Mundrander* (Pompeckj 1884; Teisseyre 1889; Mojsisovics 1886; Wähner 1894; Diener 1895); demarcation lines (Matsumoto *et al.* 1972; Obata *et al.* 1978); parabolic lines (Arkell *et al.* 1957a; Matsumoto 1991; Maeda 1993); and transitional mouth borders (Tozer 1991).

Megastriae are commonly followed by a co-marginal rib on the next segment, suggesting a relationship between pauses in secretion and rib formation (Bucher *et al.* 1996). However, based on a literature review and our large number of exceptionally well-preserved specimens from Timor, we assert that the alleged ribs of all species assigned to *Anasibirites* are in fact megastriae and not true ribs (i.e. plications) in a morphogenetic sense. True ribs in *Anasibirites* are only rarely observed, mostly on some mature body chambers devoid of megastriae.

The shape and spacing of megastriae in *Anasibirites* are directly related to the shape of the whorl section. For instance, identical and closely spaced megastriae (very short and regular growth increments) are observed on specimens of *A. multiformis* (Fig. 5A), with compressed whorls. In contrast, juvenile stages of *A. kingianus* and *A. angulosus* (with depressed whorls) exhibit irregular growth increments with megastriae of highly variable magnitude, thus mimicking the intercalation of stronger ribs (Fig. 5B–C). On the most robust species (*A. nevolini*, evolute with depressed whorls), megastriae are even more pronounced (Fig. 5D).

Measurements and multivariate analysis

Our data set includes 888 measured specimens of *Anasibirites* from the Noe Tobe block. We also included in our analyses measurements of additional specimens assigned to *A. kingianus* from the Salt Range and Spitsbergen, as well as measurements of specimens assigned to *A. multiformis* from Utah and Idaho (Fig. 2), resulting in a data set with 955 sets of measurements. All of these specimens were split into morphological groups on the basis of their similarity with the four recently validated species of *Anasibirites* (Brühwiler and Bucher 2012a; Brayard *et al.* 2013), and these groups were then statistically compared. Each set of measurements includes classical geometric parameters of the ammonoid conch such as the shell diameter (D) and corresponding whorl height (H), whorl width (W) and umbilical diameter (U). To assess the variability of these parameters for each species, the parameters are plotted as a ratio of the size-related parameter D (H/D, W/D and U/D) to remove the influence of growth. In addition to these three ratios, the ratio W/H is also plotted as a simple descriptor of the whorl section.

Box plots are constructed to illustrate the univariate distribution of the four conch ratios for each studied morphological group. These graphs display a visual comparison of the distribution of quantitative parameters with its median value (horizontal line), its 25th and 75th percentiles (the box that contains half of the values around the median), its extended interquartile range (marked by the whiskers) and its eventual outliers (isolated dots). These plots allow us to determine whether the morphological groups differ by their biometric parameters as indicated by the amount of overlap between them.

The normality of the H/D, U/D, W/D and W/H parameters is graphically assessed by means of a quantile–quantile plot and statistically tested by means of a Lilliefors test. This test evaluates the null hypothesis that the investigated data have a normal distribution with unspecified mean and variance. Results of the test are reported on the figures by a specific label: 'normal' indicates that the test cannot reject the null hypothesis of normality (at a confidence level of 95%), while 'NOT normal' indicates that the hypothesis of a normal distribution is rejected (at a type I error rate <5%). The quantile–quantile or Q–Q plot is an exploratory graphic used to check the validity of a distributional assumption for a data set. In general, the basic idea is to compute and compare the theoretically expected value for each data point based on the distribution in question. On a Q–Q plot, if the data conform to a normal distribution, the data will all lie quite close to a line. Normality of the data is also empirically evaluated by means of a standard histogram of the values. In this context, the outline of the chart is expected to closely approximate a bell shape.

The growth trajectories of H/D, W/D, U/D and W/H ratios are also explored by means of scatter diagrams and by fitting an allometric curve to the data with respect to shell diameter in order to evaluate the differences in size-based allometries of the geometry of the shell. Because allometric growth conforms to an exponential-like equation, the values of each parameter are fitted by a power equation by means of a linear regression of log-transformed data. The isometric versus allometric state is tested by a Z-test with the null hypothesis that the allometric exponent is equal to 1 (i.e. isometric growth) at a confidence level of 95%.

Finally, a linear discriminant analysis (LDA) has been performed in order to graphically evaluate how the studied morphotypes of *Anasibirites* can be more or less well distinguished based on the four ratios H/D, U/D, W/D and W/H. Briefly, the purpose of this standard ordination method is to project the multidimensional data set (composed here of the four conch ratios) onto newly constructed axes, which maximize the discrimination between given groups (here, the *Anasibirites* morphotypes) and which are ordered by decreasing importance. This method is thus a convenient tool for finding differences between groups (taxa) in the function of the parameters and of the value of each parameter. This method enables investigation of the patterns of morphological variation in the studied species or morphological groups.

The descriptive, exploratory and multivariate analyses of the biometric ratios have been performed with the free scientific and statistical environment R version 3.0.3 (R Core Team 2014) and with the package epaleo (CM unpub.). Additional details on the methods are found in Reyment and Savazzi (1999), Davis (2002) and Hammer and Harper (2006), among others.

DISCUSSION

Comparison between A. kingianus *and* A. nevolini

Waagen (1895) erected *A. kingianus* for specimens with indistinct ventral shoulders and an arched venter (Figs 4, 6–9, 10A–M). In juvenile stages, the whorl section is somewhat quadratic and the venter is separated from the flanks by angular shoulders (Waagen 1895). This juvenile stage is well documented in cross-sections (Fig. 11). Furthermore, according to Waagen (1895, p. 108), ornamentation of the juvenile stages consists of 'very unequal, somewhat falciform ribs' with 'eight to ten strong ribs on one volution and between these some three or four weaker ones intercalated and showing the same curve' (see Fig. 10A–M). On mature specimens, 'the sculpture becomes somewhat different' with 'ribs all of equal strength'.

The description of *A. kingianus* by Waagen (1895) is very close to that of *A. nevolini* Zakharov, 1968 in Brayard and Bucher (2008, p. 58). These authors described *A. nevolini* with a subtabulate-to-tabulate venter and a 'regular alternation of concave, weak and strong ribs', as well as with ornamentation 'somewhat attenuated on adult specimens'. The Timor specimens tentatively assigned to *A. nevolini* (Fig. 12) based on Brayard and Bucher (2008) are mostly small specimens (<30 mm), and their sculpture, although slightly more pronounced, is very similar to that of juvenile specimens assigned here to *A. kingianus* (Fig. 10A–M).

According to Brayard and Bucher (2008), *A. nevolini* is more evolute than all other congeneric species. However, the statistical comparisons of the measurements of our Timor specimens provisionally assigned to *A. kingianus* and *A. nevolini* (747 and 40, respectively) show that specimens of *A. nevolini* are not more evolute than juvenile specimens of *A. kingianus* (Fig. 13: U/D). These latter only show a slightly less pronounced sculpture (Fig. 10A–M). The LDA also indicates that *A. nevolini* and juveniles of *A. kingianus* occupy the same portion of morphospace (Fig. 14). The two outliers of *A. nevolini* shown in the LDA are extremely thick variants (e.g. Fig. 12K). Finally, *A. nevolini* and *A. kingianus* share the same whorl geometry in their juvenile stages (Fig. 11).

Anasibirites nevolini therefore represents the robust and 'paedomorphic' end-member variant of *A. kingianus*. This 'nevolini' variant includes specimens of *A. kingianus* that display an extension and/or accentuation of the robust early juvenile stages (Fig. 12; Brayard and Bucher 2008, pl. 28, figs 7–8). Specimens of the 'nevolini' variant with the most robust sculpture are also more evolute (Fig. 12A,

FIG. 6. *Anasibirites kingianus* (Waagen, 1895) from Noe Tobe (Timor). A, PIMUZ 31419. B, suture line of PIMUZ 31420 with scale bar representing 5 mm, at H = 20 mm. C, PIMUZ 31421. D, PIMUZ 31422. E, PIMUZ 31423. F, PIMUZ 31424. G, PIMUZ 31425. Stars indicate the position of last septum; H, whorl height. Scale bar for A, C–G represents 10 mm.

FIG. 7. *Anasibirites kingianus* (Waagen, 1895) from Noe Tobe (Timor). A, PIMUZ 31411. B, PIMUZ 31412. C, PIMUZ 31413. D, PIMUZ 31414. E, PIMUZ 31415. F, PIMUZ 31416. G, PIMUZ 31417. H, PIMUZ 31418. Star indicates the position of last septum. Scale bar represents 10 mm.
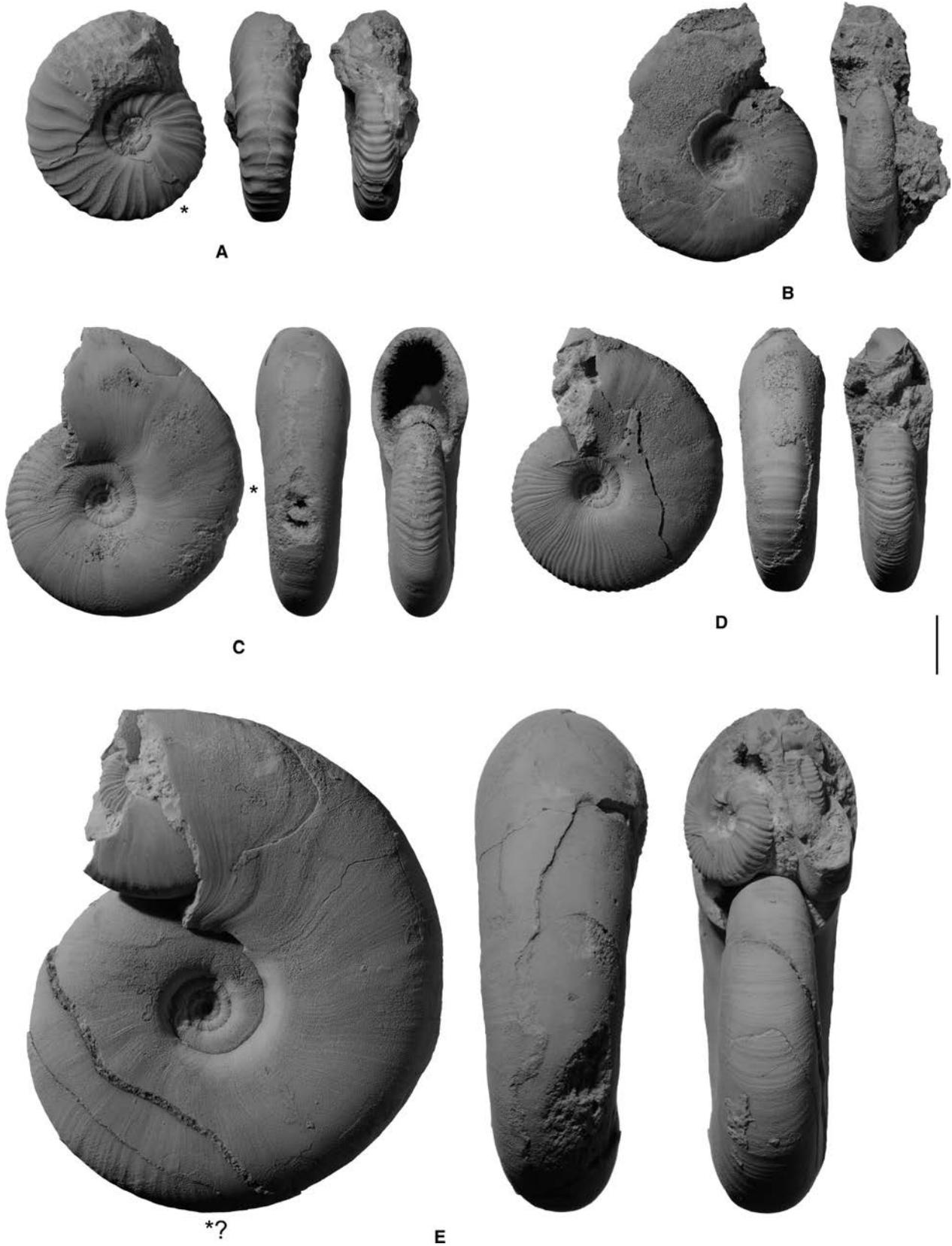
FIG. 8. *Anasibirites kingianus* (Waagen, 1895) from Noe Tobe (Timor). A, PIMUZ 31428. B, PIMUZ 31429. C, PIMUZ 31430. D, PIMUZ 31431. E, PIMUZ 31432. Stars indicate the position of last septum. Scale bar represents 10 mm.

FIG. 9. *Anasibirites kingianus* (Waagen, 1895) from Noe Tobe (Timor). A, PIMUZ 31433. B, PIMUZ 31434. C, PIMUZ 31435. D, PIMUZ 31436. E, PIMUZ 31437. Stars indicate the position of last septum. Scale bar represents 10 mm.
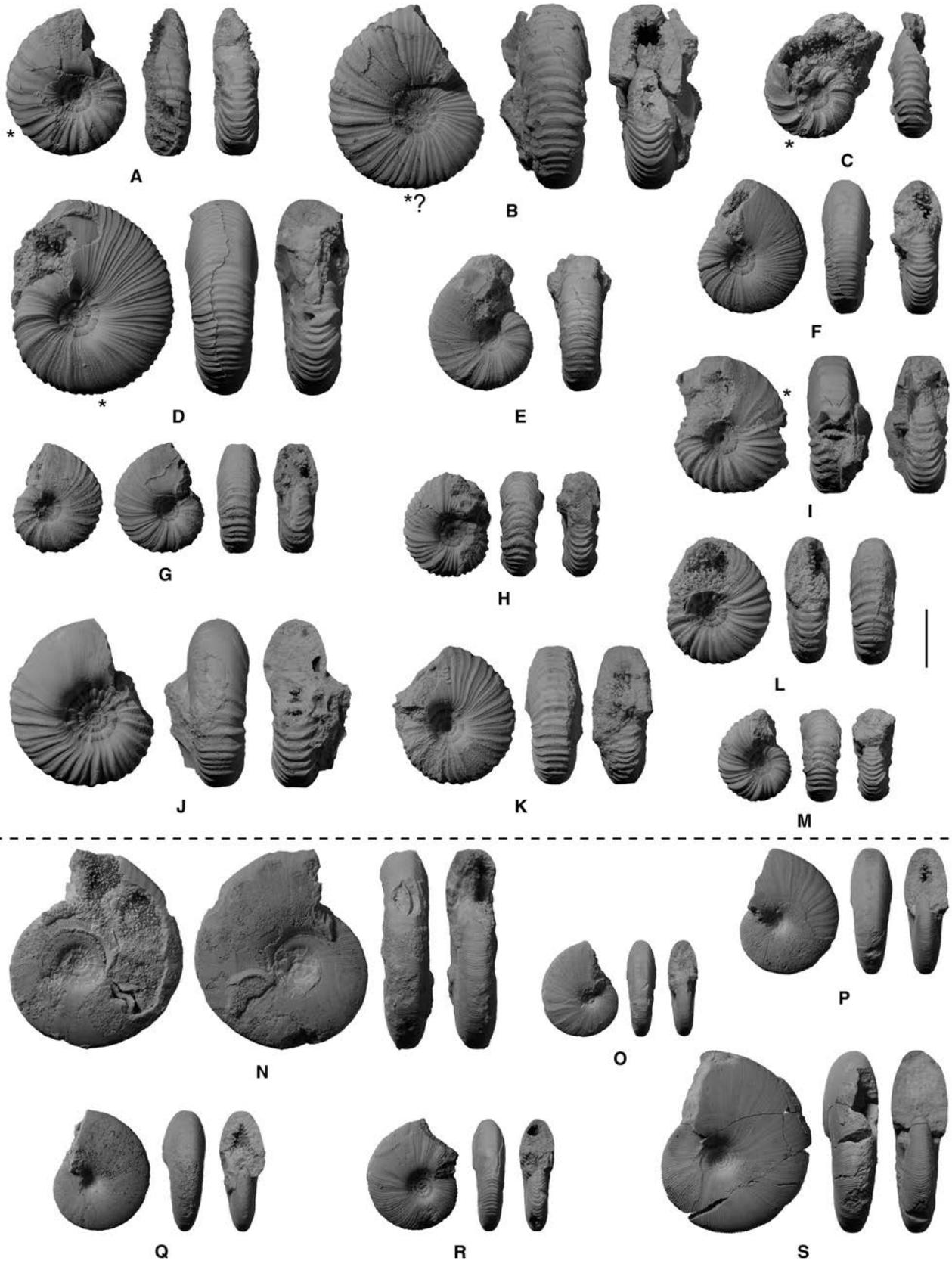
FIG. 11. Schematic whorl sections of specimens of *Anasibirites kingianus* (Waagen, 1895) and *A. multiformis* Welter, 1922 from Noe Tobe (Timor). From left to right: PIMUZ 31432, PIMUZ 31419, PIMUZ 31456, PIMUZ 31468, PIMUZ 31477, PIMUZ 31499, PIMUZ 31396. Scale bar represents 10 mm.
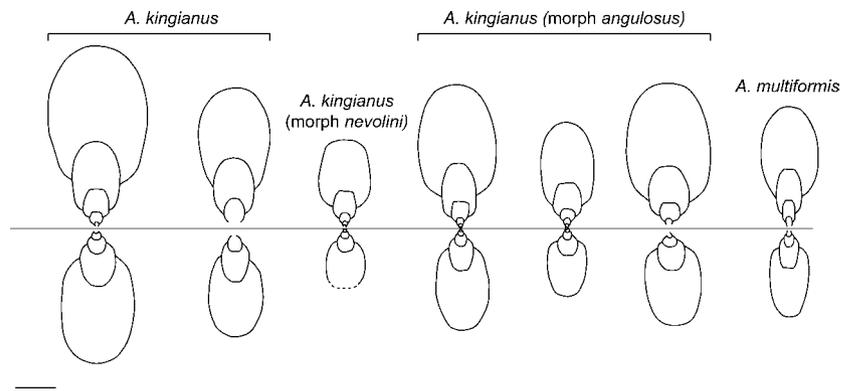
G, K). This type of covariation conforms to the well-known Buckman's first law of covariation (Westermann 1966). For a review of ammonoid intraspecific variability in general and Buckman's rules of covariation, see De Baets *et al.* (2015) and Monnet *et al.* (2015).

In conclusion, *A. nevolini* does not show any diagnostic differences with respect to *A. kingianus*. Consequently, *A. nevolini* is here synonymized with *A. kingianus*.

Comparison between A. kingianus *and* A. angulosus

According to Brühwiler and Bucher (2012*a*) and Brayard *et al.* (2013), *A. kingianus* is mainly distinguished by its arched venter with rounded shoulders, which is in agreement with the original description of Waagen (1895). However, as previously mentioned, the juvenile stages of *A. kingianus* are characterized by a somewhat quadratic whorl section and a venter separated from the flanks by angular shoulders (Waagen 1895).

Anasibirites angulosus was erected by Waagen (1895) who distinguished this species from *A. kingianus* by 'angular whorls retained by it in more advanced stages of growth' and 'ribs that show an angular bend in the middle of the external part' (Waagen 1895, p. 119). According to Waagen's (1895, p. 118) original description of *A. angulosus*, the whorl section of juvenile stages is somewhat quadratic, the venter is separated from the flanks by angular shoulders and the 'ribs' are very unequal in strength with generally two fainter 'ribs' intercalated between two stronger ones. Based on this information and plates from Waagen (1895) and Brühwiler and Bucher (2012*a*), we tentatively assigned

80 specimens to *A. angulosus* (Figs 15–17). Brayard *et al.* (2013) also figured specimens as *Anasibirites* cf. *angulosus*. However, these specimens do not exhibit true megastriae, but instead, bear true ribs. Therefore, these specimens are not representative of the genus *Anasibirites* and more likely belong to the genera *Hemiprionites* or *Arctoprionites*.

Based on Timor specimens tentatively assigned to *A. angulosus* and following Waagen's descriptions, the juvenile stages of *A. kingianus* and *A. angulosus* are nearly identical. Both species display juvenile stages with a somewhat quadratic whorl section, angular shoulders and megastriae of highly variable magnitude (Figs 5B–C, 11). Considering the extreme variability of the shape of megastriae within *Anasibirites*, the presence of megastriae in *A. angulosus* that exhibit an angular bend in the middle of the flank (Waagen 1895) is unlikely to be a diagnostic character. Consequently, *A. angulosus* may only be distinguished from *A. kingianus* by 'angular whorls retained by it in more advanced stages of growth' (Waagen 1895, p. 119).

It should be noted that the type material of *A. angulosus* is represented by two rather small specimens (<25 mm). Thus, the character 'angular whorls retained by it in more advanced stages of growth' (Waagen 1895, p. 119) is not relevant for the type material. However, *A. angulosus* was also described by Brühwiler and Bucher (2012*a*) as having a tabulate venter with angular shoulders, becoming slightly rounded on outer whorls.

Our large sample of *A. kingianus* specimens includes many intermediate morphs that range between an arched venter with rounded shoulders and a tabulate venter with angular shoulders (Fig. 18). Specimens of *A. kingianus*

FIG. 10. A–M, juvenile specimens of *Anasibirites kingianus* (Waagen, 1895) from Noe Tobe (Timor); A, PIMUZ 31438; B, PIMUZ 31439; C, PIMUZ 31440; D, PIMUZ 31441; E, PIMUZ 31442; F, PIMUZ 31443; G, PIMUZ 31444; H, PIMUZ 31445; I, PIMUZ 31446; J, PIMUZ 31447; K, PIMUZ 31448; L, PIMUZ 31449; M, PIMUZ 31450. N–S, *Anasibirites multiformis* Welter, 1922 from Noe Tobe (Timor); N, PIMUZ 31389; O, PIMUZ 31390; P, PIMUZ 31391; Q, PIMUZ 31392; R, PIMUZ 31393; S, PIMUZ 31394. Stars indicate the position of last septum. Scale bar represents 10 mm.
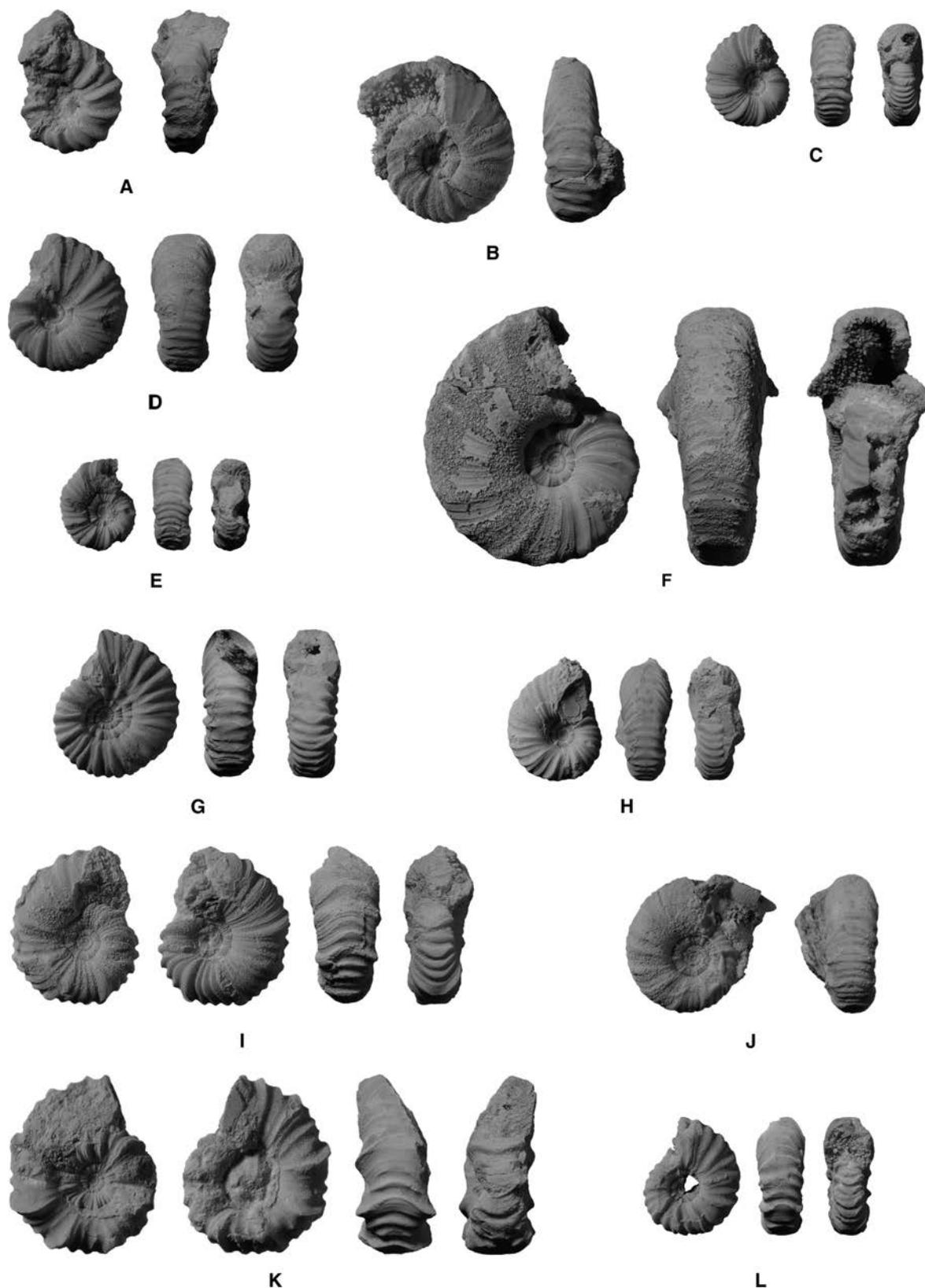
FIG. 12. *A. kingianus* (morph *nevolini*) (Waagen, 1895) from Noe Tobe (Timor). A, PIMUZ 31451. B, PIMUZ 31452. C, PIMUZ 31453. D, PIMUZ 31454. E, PIMUZ 31455. F, PIMUZ 31456. G, PIMUZ 31457. H, PIMUZ 31458. I, PIMUZ 31459, X2. J, PIMUZ 31460. K, PIMUZ 31461, X2. L, PIMUZ 31462. Scale bar represents 10 mm.
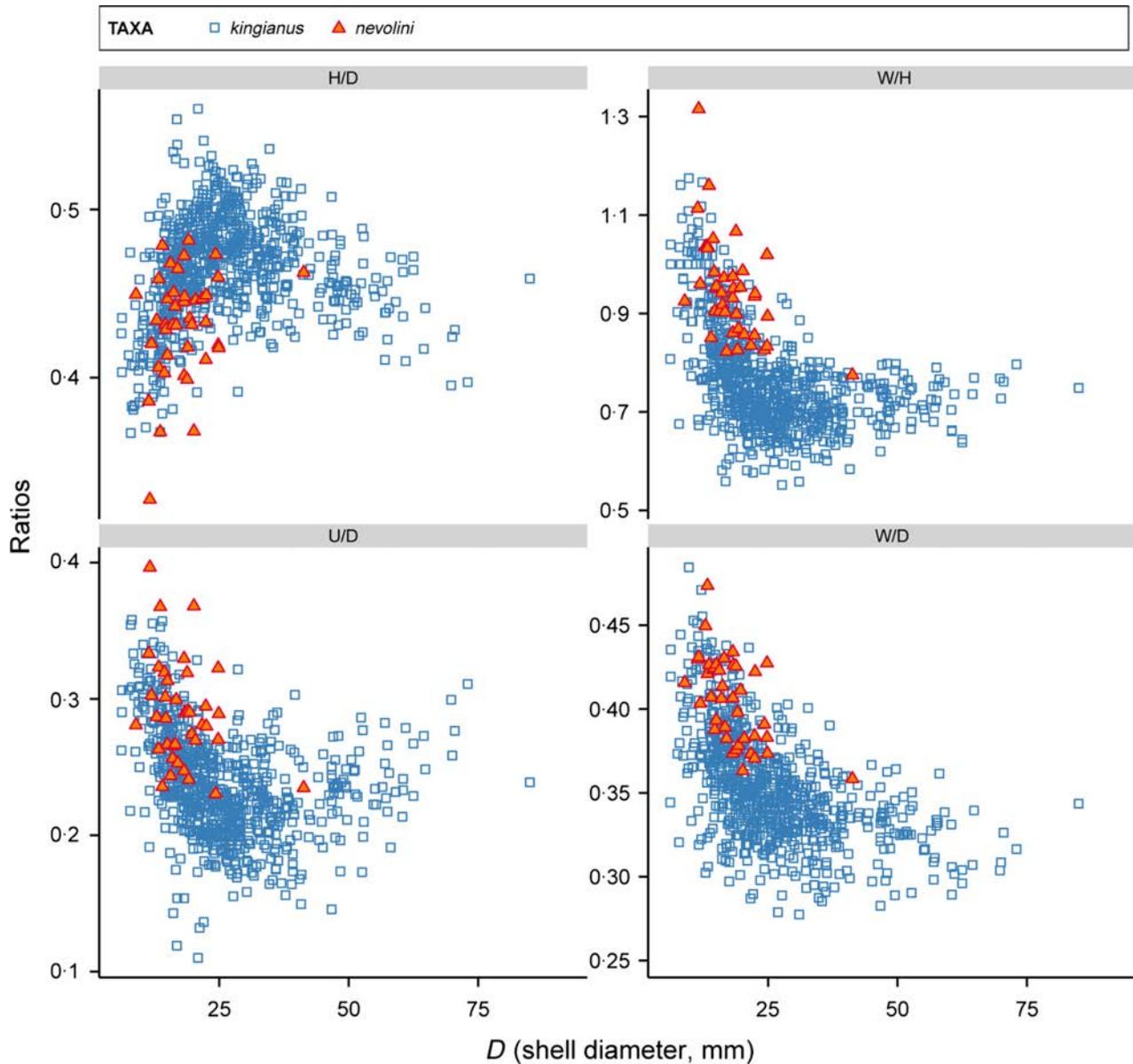
FIG. 13. Scatter diagrams of H/D, W/D, U/D and W/H for *Anasibirites kingianus* (Waagen 1895) and *A. kingianus* (morph *nevolini*) from Noe Tobe (Timor). D, shell diameter; H, whorl height; W, whorl width; U, umbilical diameter.

with a subtabulate venter with marked shoulders are thus representative of intermediate variants between *A. angulosus* and *A. kingianus* (Fig. 18). The presence of a tabulate venter with angular shoulders therefore is probably not a reliable diagnostic character.

Additionally, the statistical comparisons of the measurements of our specimens provisionally assigned to *A. angulosus* and *A. kingianus* indicate that the two species cannot be differentiated based on their classical biometric parameters (Figs 14, 19–20; the distributions of the two species largely overlap in the LDA). Brühwiler and Bucher (2012a) also mentioned that the ribs on adult

specimens of *A. angulosus* sometimes thicken at midflank, forming elongated tubercles. However, this feature is too rarely observed to be used as a diagnostic character.

Thus, it appears that *A. angulosus* is only a variant of *A. kingianus*. As with the variant '*nevolini*', the variant '*angulosus*' results from an extreme ontogenetic variation of *A. kingianus*. This variant corresponds to specimens of *A. kingianus* that display an extension and/or accentuation of the tabulate and angular venter of their juvenile stages to later stages. It is worth noting that the outer whorl of large specimens of the variant '*angulosus*'
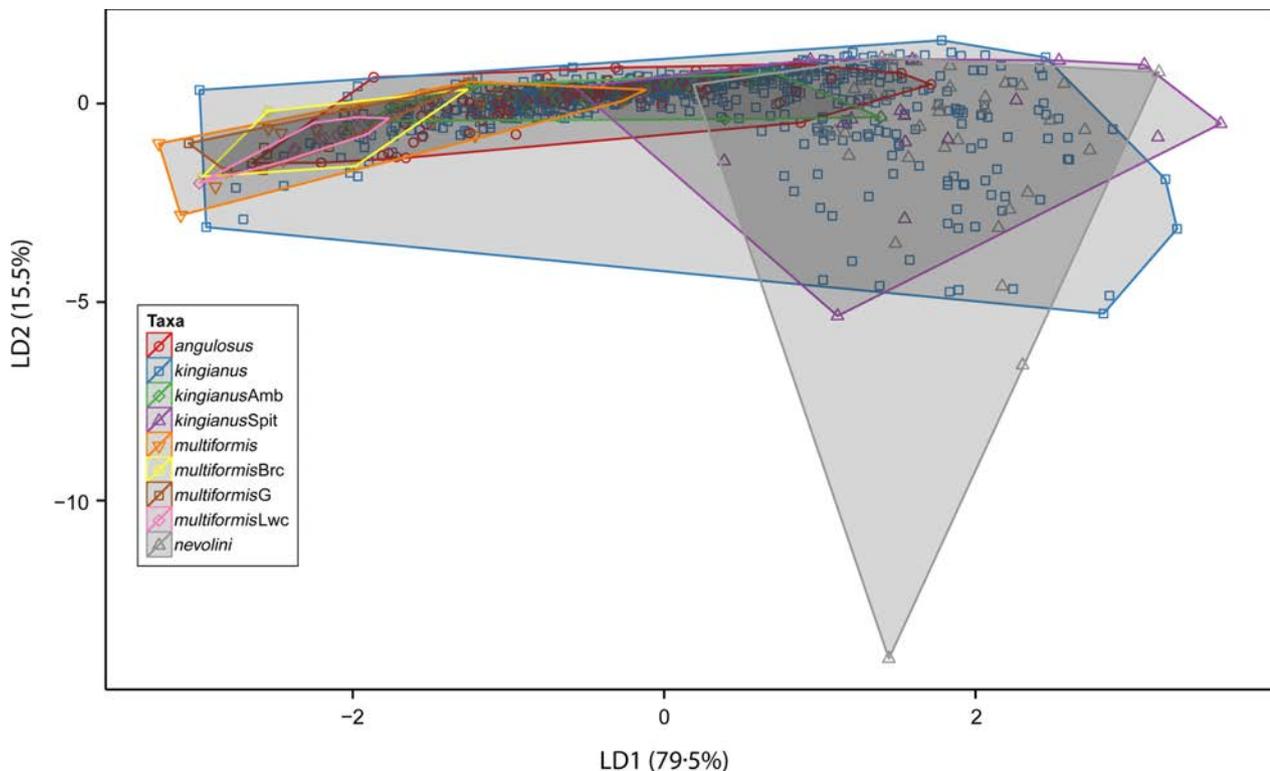
FIG. 14. Linear discriminant analysis based on the four shell ratios H/D, W/D, U/D and W/H for the morphotypes of *A. kingianus* (Waagen, 1895), *A. kingianus* (morph *angulosus*), *A. kingianus* (morph *nevolini*) and *A. multiformis* Welter, 1922 (biplot with convex hull of the taxa). Specimens from Noe Tobe (Timor): 'angulosus', 'kingianus', 'multiformis' and 'nevolini'; specimens from Pakistan: 'kingianusAmb'; specimens from Utah/Idaho: 'multiformisBrc', 'multiformisG' and 'multiformisLwc'; specimens from Spitsbergen: 'kingianusSpit'. The first and second discriminant axes account for about 95% of the total variation. The first axis is mostly controlled by the most common values of the W/H and W/D ratios, with the highest values (depressed whorls) towards the right and the lowest values (compressed whorls) towards the left. The second axis is also mostly controlled by the W/H and W/D ratios, but this is due to the extreme marginal values; highest values (depressed whorls) towards the bottom and lowest values (compressed whorls) towards the top. The restricted morphospace occupied by *A. multiformis* reflects its nearly isometric growth, whereas *A. kingianus* (all variants included) occupies a very large space reflecting its allometric growth, which induces larger morphological changes and intraspecific variation. D, shell diameter; H, whorl height; W, whorl width; U, umbilical diameter.

displays true ribs, more pronounced on the venter than on the flanks (e.g. Figs 15F, 16B, F).

Highly variable ornamentation also exists in the 'angulosus' variant. Evolute specimens exhibit megastriae of high magnitude (e.g. Figs 15D, H, 17H), while some involute specimens exhibit lower-magnitude megastriae (Fig. 17A–D).

In conclusion, *A. angulosus* does not show any diagnostic differences with respect to *A. kingianus*. Consequently, *A. angulosus* is here synonymized with *A. kingianus*.

Comparison between A. kingianus *and* A. multiformis

Anasibirites multiformis (Figs 10N–S, 21–23) was erected by Welter (1922), but it was recently redefined by Brayard and Bucher (2008, p. 57). According to the latter authors, *A. multiformis* is characterized by 'a

tabulate-to-subtabulate venter and an identical ornamentation at all developmental stages consisting of dense, concave, forward projected growth lines (striae) with very few distinct ribs' (see also Brühwiler and Bucher 2012b).

Well-preserved specimens from Timor assigned to *A. multiformis* (Figs 10N–S, 21) reveal that the growth lines described by Brayard and Bucher (2008) for *A. multiformis* are actually very low-magnitude, thin and closely spaced megastriae.

Specimens assigned to *A. multiformis* differ from *A. kingianus* by their very low-magnitude megastriae on early whorls, whereas variants of *A. kingianus* all exhibit megastriae of highly variable magnitude on their inner whorls (Fig. 5). At the mature stage, specimens assigned to *A. multiformis* retain the same sculpture (e.g. Figs 22C, 23A–B; as described in Brayard and Bucher 2008) consisting of very low-magnitude megastriae, whereas mature

FIG. 15. *Anasibirites kingianus* (morph *angulosus*) (Waagen, 1895) from Noe Tobe (Timor). A, PIMUZ 31463. B, PIMUZ 31464. C, PIMUZ 31465. D, PIMUZ 31466. E, PIMUZ 31467. F, PIMUZ 31468. G, PIMUZ 31469. H, PIMUZ 31470. I, PIMUZ 31471. J, PIMUZ 31472. K, PIMUZ 31473. Stars indicate the position of last septum. Scale bar represents 10 mm.
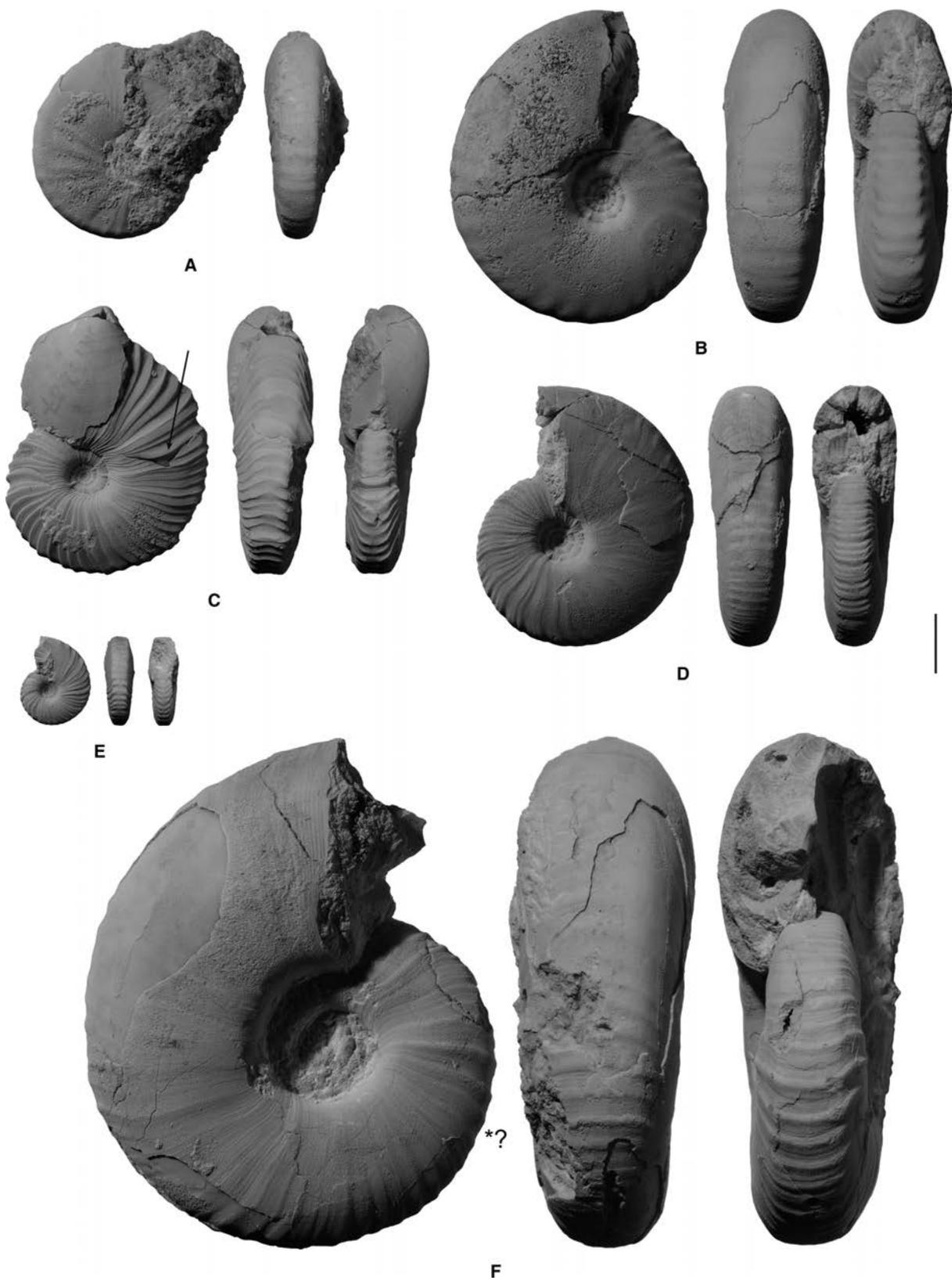
FIG. 16. *Anasibirites kingianus* (morph *angulosus*) (Waagen, 1895) from Noe Tobe (Timor). A, PIMUZ 31474. B, PIMUZ 31475. C, PIMUZ 31476. D, PIMUZ 31477. E, PIMUZ 31478. F, PIMUZ 31479. Arrow indicates a repaired injury. Star indicates the position of last septum. Scale bar represents 10 mm.
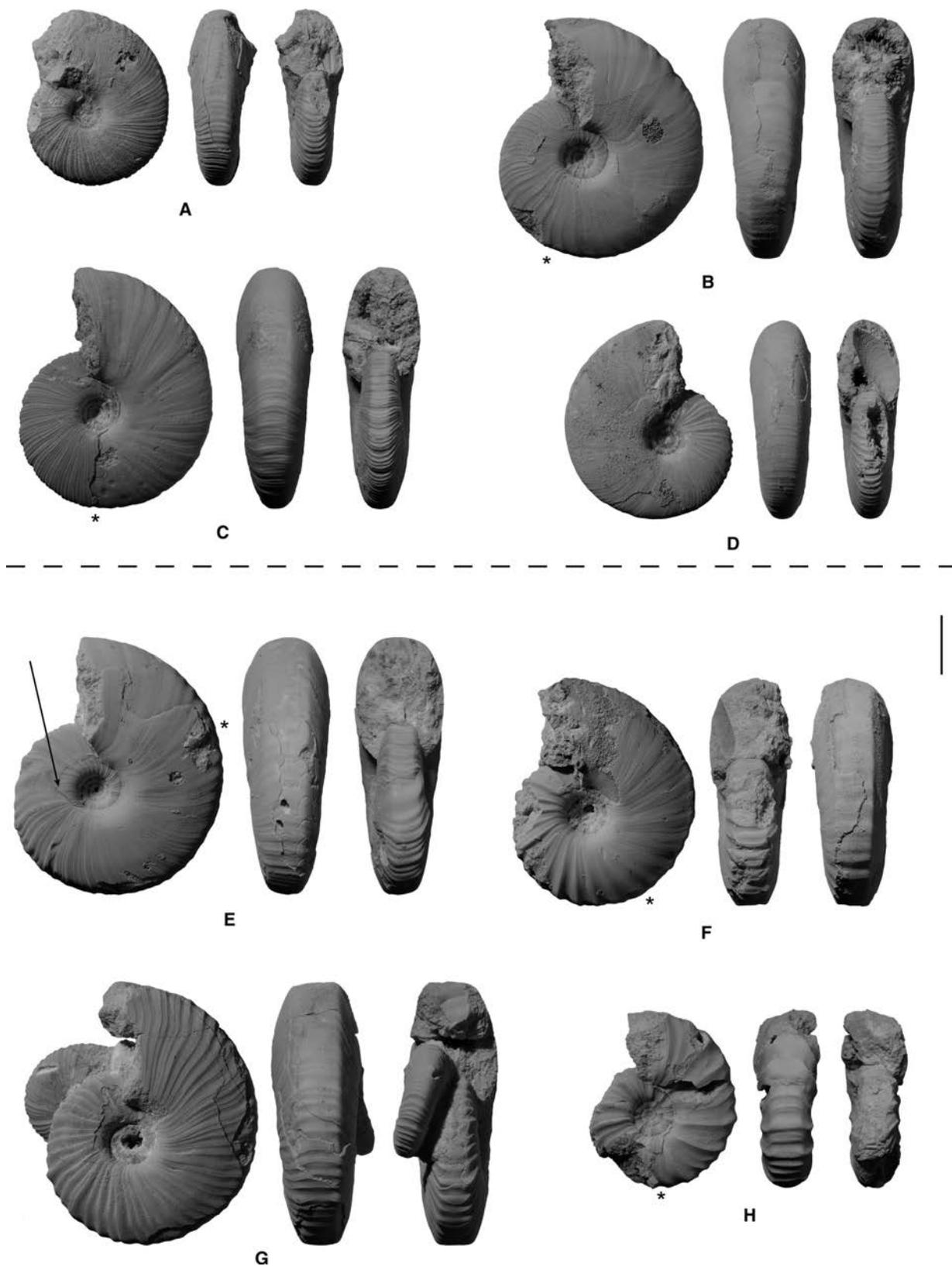
FIG. 17. *Anasibirites kingianus* (morph *angulosus*) (Waagen, 1895) from Noe Tobe (Timor). A–D, specimens with low-magnitude megastriae. A, PIMUZ 31480. B, PIMUZ 31481. C, PIMUZ 31482. D, PIMUZ 31483. E, PIMUZ 31484. F, PIMUZ 31485. G, PIMUZ 31486. H, PIMUZ 31487. Arrow indicates a repaired injury. Stars indicate the position of last septum. Scale bar represents 10 mm.

FIG. 18. *Anasibirites kingianus* (Waagen, 1895) from Noe Tobe (Timor). Specimens with subtabulate venter with marked shoulders. A, PIMUZ 31488. B, PIMUZ 31489. C, PIMUZ 31490. D, PIMUZ 31491. E, PIMUZ 31492. F, PIMUZ 31493. G, PIMUZ 31494. H, PIMUZ 31495. I, PIMUZ 31496. J, PIMUZ 31497. K, PIMUZ 31498. Stars indicate the position of last septum. Scale bar represents 10 mm.
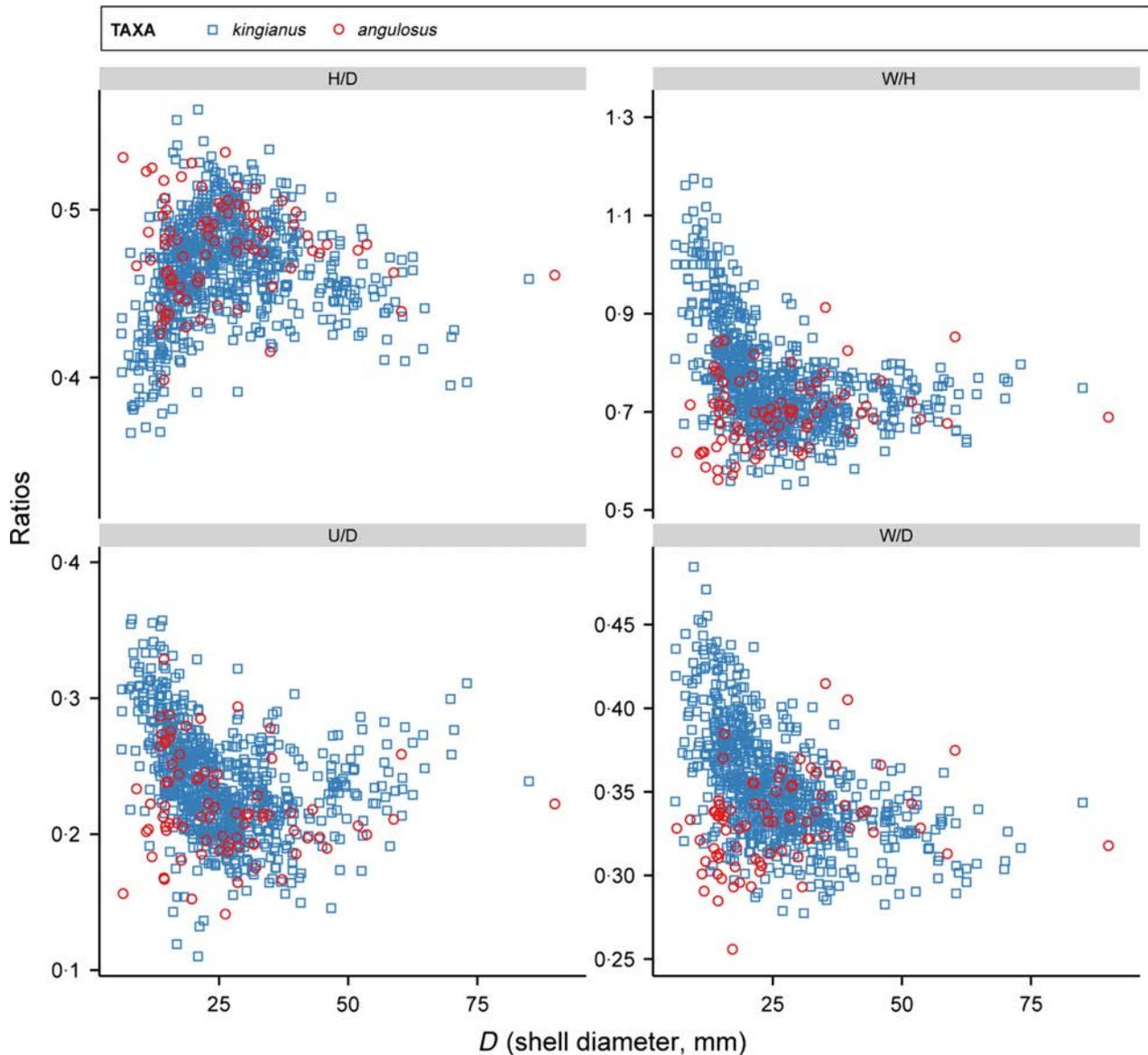
FIG. 19. Scatter diagrams of H/D, W/D, U/D and W/H for *Anasibirites kingianus* (Waagen, 1895) and *Anasibirites kingianus* (morph *angulosus*) from Noe Tobe (Timor). D, shell diameter; H, whorl height; W, whorl width; U, umbilical diameter.

specimens of *A. kingianus* exhibit a shell without megastriae but with growth lines and ribs (more pronounced on the venter) on some specimens.

Whorl sections indicate that the difference in megastriae on the inner whorls (Fig. 5) results from diverging growth trajectories. Early stages of *A. multiformis* are indeed characterized by compressed whorls, whereas early stages of *A. kingianus* (including the variants 'nevolini' and 'angulosus') are characterized by somewhat quadratic whorls (Fig. 11). This is also accompanied by an allometric growth for *A. kingianus* and nearly isometric growth for *A. multiformis* (Fig. 24). The nearly isometric growth of *A. multiformis* thus stands as a reliable diagnostic feature for this species.

Shape and spacing of megastriae are directly related to the shape of the whorl section. The more compressed the whorls, the less pronounced the megastriae. The nearly isometric growth of *A. multiformis* therefore produces megastriae with a constant shape throughout ontogeny. Some extremely rare specimens of *A. multiformis* exhibit a few megastriae of slightly higher magnitude on their early whorls (e.g. Fig. 10N). However, these specimens never display megastriae of highly variable magnitude such as those of *A. kingianus*, and nevertheless, they also display dense megastriae of very low magnitude on outer whorls. In most cases, the presence of megastriae of unusually slightly higher magnitude on the early whorls of some specimens of
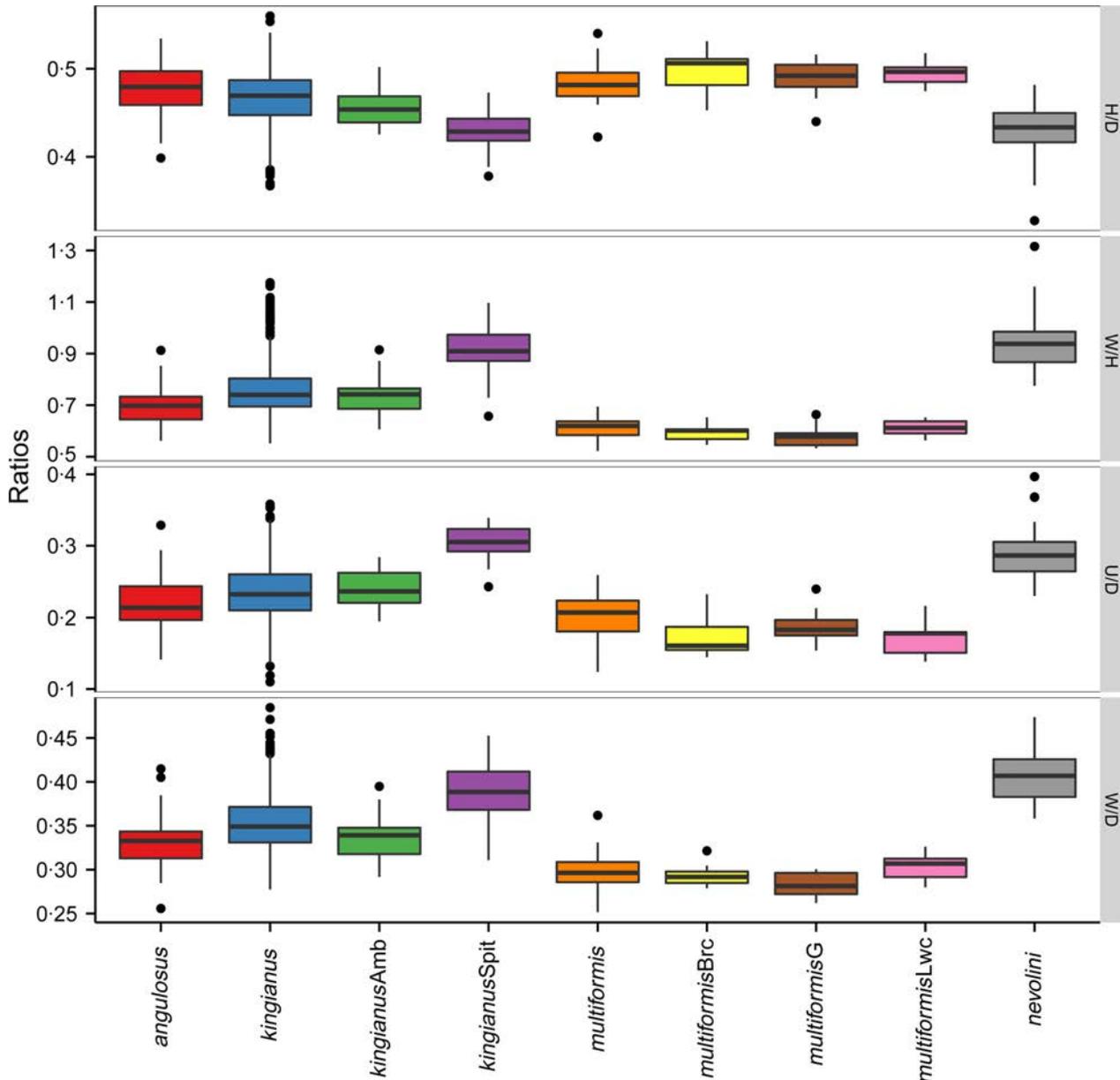
FIG. 20. Box plots of H/D, W/D, U/D and W/H for all morphological groups. Specimens from Noe Tobe (Timor): '*angulosus*', '*kingianus*', '*multiformis*' and '*nevolini*'; specimens from Pakistan: '*kingianus*Amb'; specimens from Utah/Idaho: '*multiformis*Brc', '*multiformis*G' and '*multiformis*Lwc'; specimens from Spitsbergen: '*kingianus*Spit'. The boxes represent the interquartile range (i.e. the values ranging from the first to third quartiles, which are the 25th and 75th percentiles, respectively); the whiskers extend from their respective hinge to the value of 1.5× interquartile range. D, shell diameter; H, whorl height; W, whorl width; U, umbilical diameter.

A. multiformis can be explained by their unusually evolute morphology (following Buckman's first law of covariation; Fig. 10N).

With regard to statistical comparisons, the American specimens of *A. multiformis* provided additional mea-surements, especially of larger specimens (>50 mm; Figs 22–23).

As shown in Figures 20 and 25, *A. multiformis* pos-sesses the most compressed whorls. Due to its extreme intraspecific variation, the morphospace of *A. kingianus*

FIG. 21. *Anasibirites multiformis* Welter, 1922 from Noe Tobe (Timor). A, PIMUZ 31395. B, PIMUZ 31396. C, PIMUZ 31397. D, PIMUZ 31398. E, PIMUZ 31399. F, PIMUZ 31400. G, PIMUZ 31401. H, suture lines from sample PIMUZ 31397 with scale bar repre-senting 5 mm at H = 15 mm. I, PIMUZ 31402. J, PIMUZ 31403, K, PIMUZ 31404. Arrows represent repaired injury (A) or weak rib-bing (B–C). Stars indicate the position of last septum; H, whorl height. Scale bar for A–G, I–K represents 10 mm.
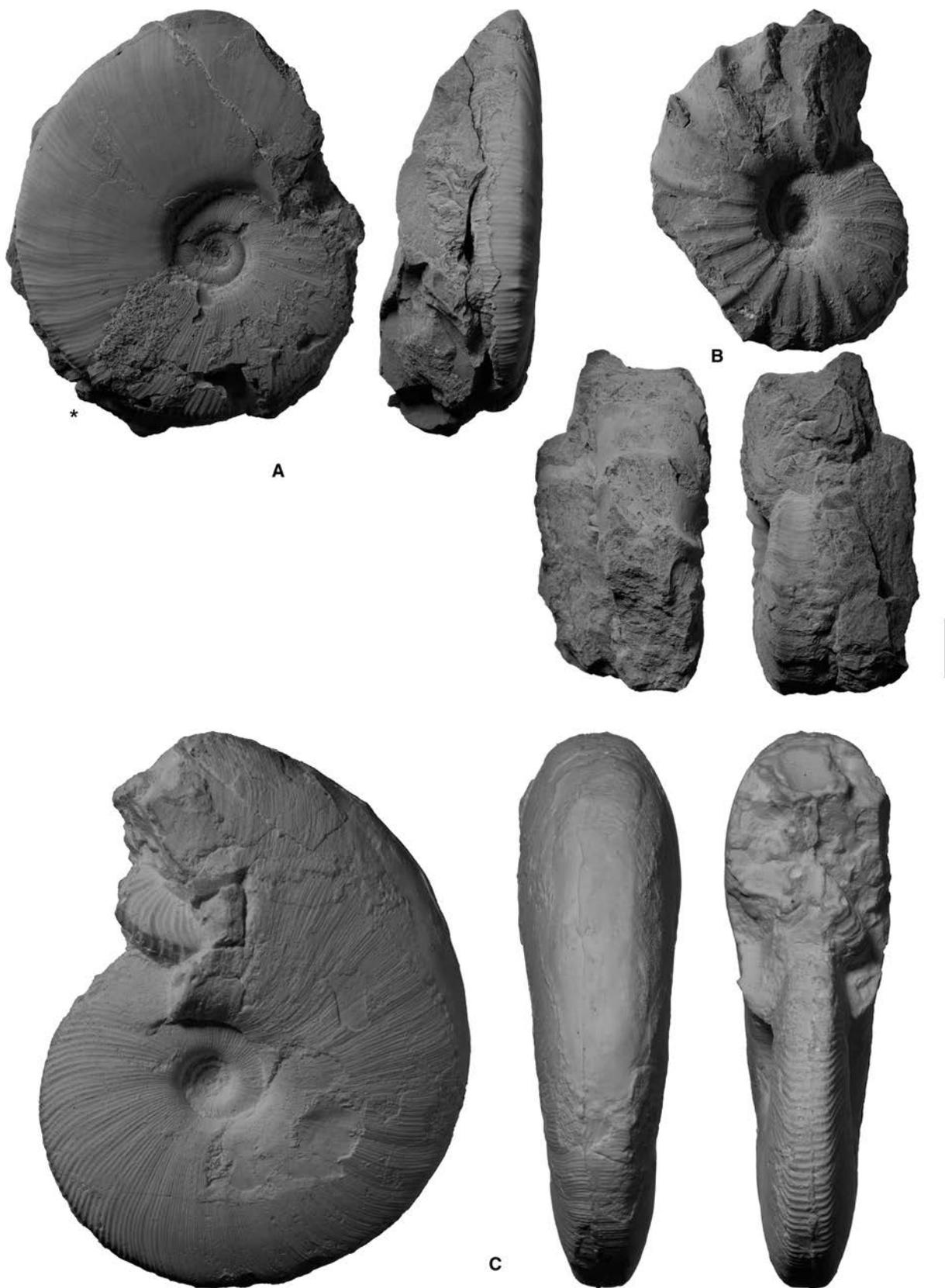
FIG. 22. *Anasibirites multiformis* Welter, 1922 from Georgetown (Idaho), except for B (Lower Weber Canyon, Utah). A, PIMUZ 31405. B, JJ2474C. C, JJ146C (cast). Star indicates the position of last septum. Scale bar represents 10 mm.
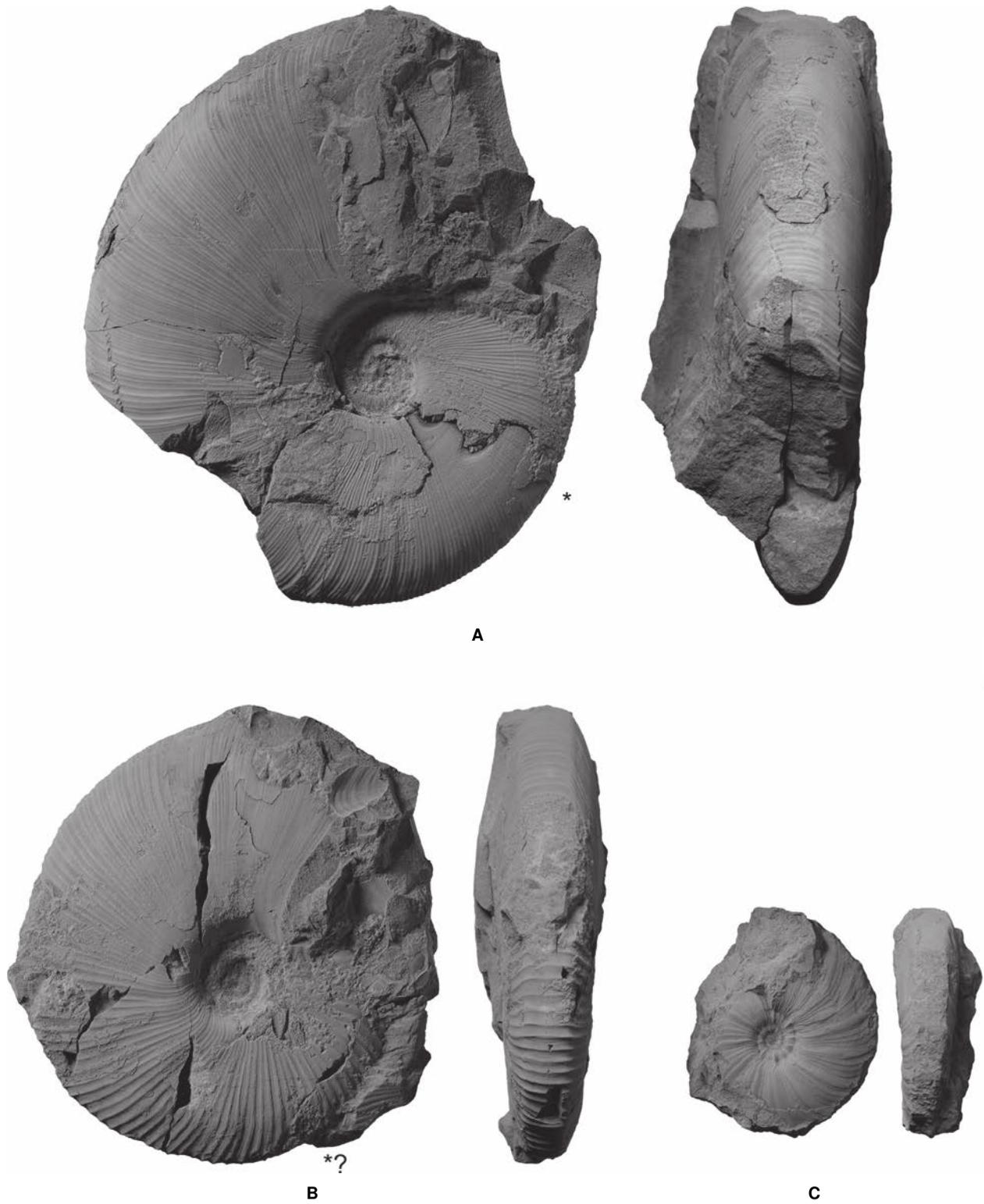
FIG. 23. *Anasibirites multiformis* Welter, 1922 from Georgetown (Idaho), except for C (Lower Weber Canyon, Utah). A, PIMUZ 31408. B, PIMUZ 31409. C, JJ2475C. Stars indicate the position of last septum. Scale bar represents 10 mm.
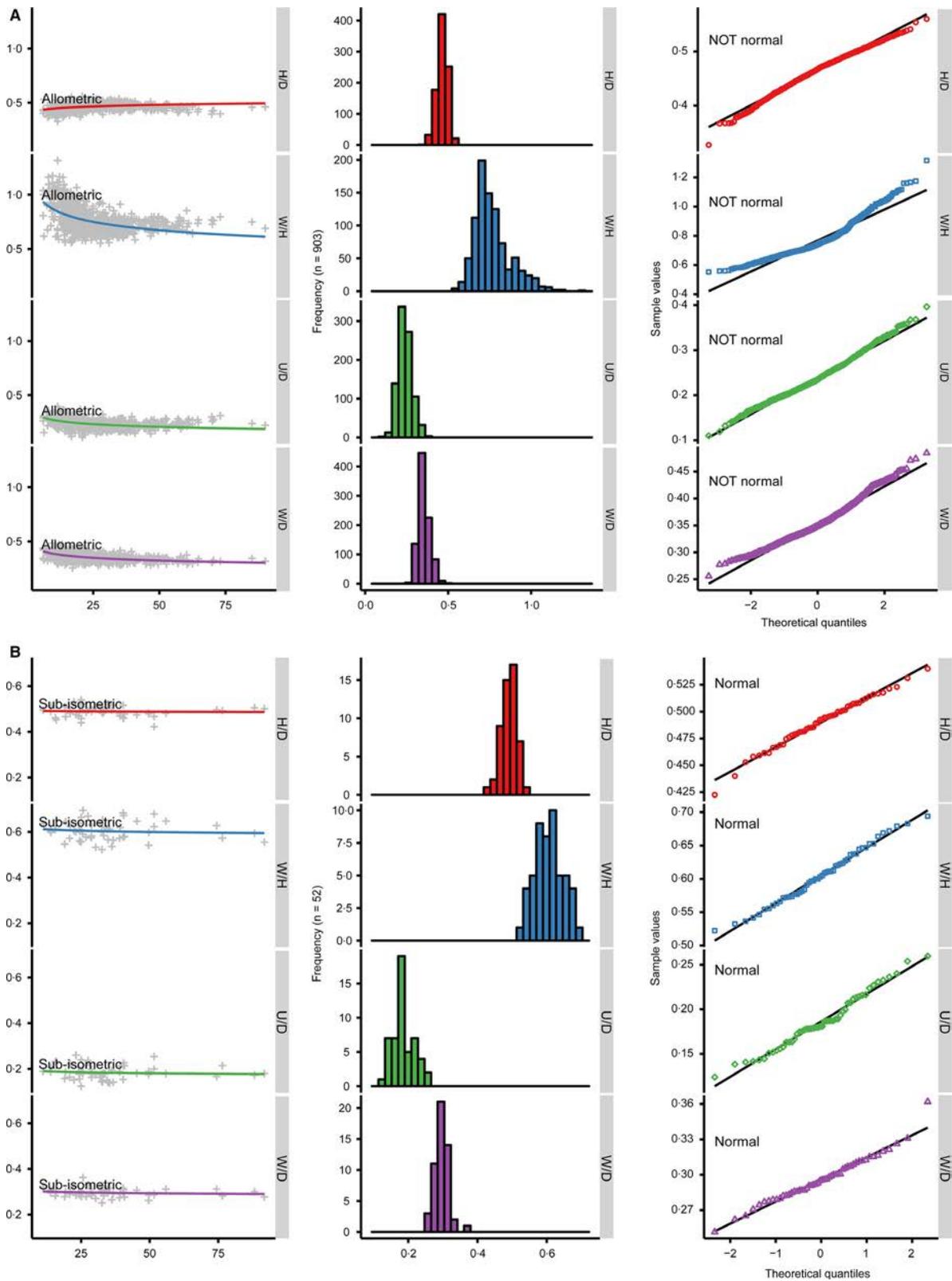
FIG. 24. Scatter diagrams with calculated allometric curves superimposed, histograms and quantile–quantile plots of H/D, W/D, U/D and W/H. A, *Anasibirites kingianus* (Waagen, 1895) all variants included. B, *A. multiformis* Welter, 1922. See text for explanation of these plots and evaluation of allometry and normality of H/D, W/D, U/D and W/H. D, shell diameter; H, whorl height; W, whorl width; U, umbilical diameter.
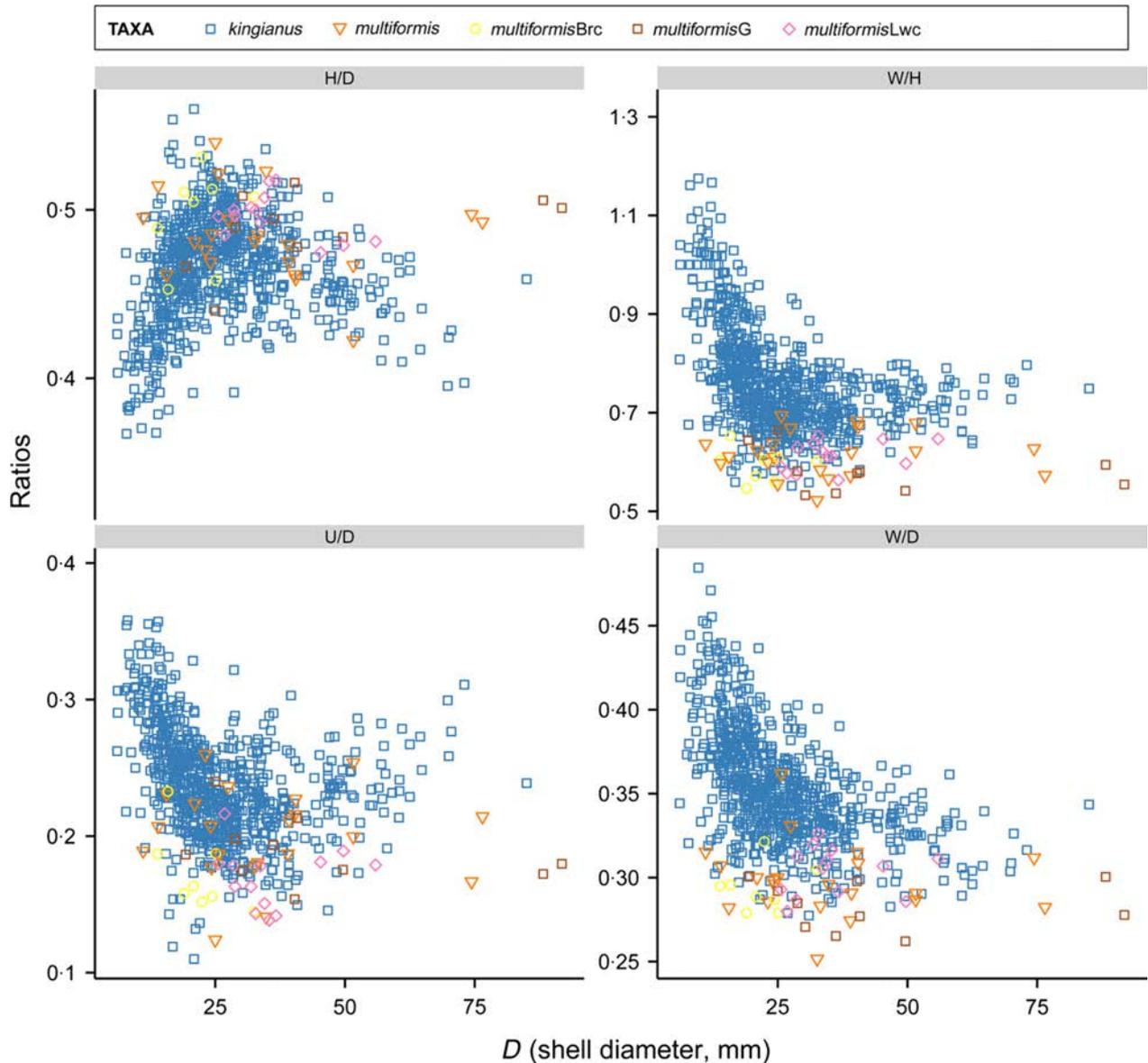
FIG. 25. Scatter diagrams of H/D, W/D, U/D and W/H for *Anasibirites kingianus* (Waagen, 1895) from Noe Tobe (Timor) and *A. multiformis* Welter, 1922 from Noe Tobe (Timor) and American localities. Specimens from Noe Tobe (Timor): '*kingianus*', '*multiformis*'; specimens from Utah/Idaho: '*multiformis*Brc', '*multiformis*G' and '*multiformis*Lwc'. D, shell diameter; H, whorl height; W, whorl width; U, umbilical diameter.

overlaps that of *A. multiformis* (Fig. 14). However, the morphospace of *A. multiformis* (all localities included) represents a distinctive subset. The compressed shell shape of *A. multiformis* at all growth stages is taken as a diagnostic character to validate this species. Adult specimens of *A. multiformis* also seem to be slightly more involute than adult specimens of *A. kingianus* (Fig. 25: U/D).

Finally, *A. kingianus* mainly differs from *A. multiformis* by: (1) its strong allometric growth characterized by quadratic early whorls and compressed mature whorls

(Fig. 24); (2) megastriae of highly variable magnitude on early whorls (Fig. 5B–D); and (3) mature whorls without megastriae, but with growth lines and ribs (more pronounced on the venter) on some specimens. As for *A. multiformis*, its nearly isometric growth (Fig. 24) is characterized by compressed whorls and closely and regularly spaced low-magnitude megastriae from early whorls to maturity.

It should be noted that a few involute specimens of *A. kingianus* belonging to the variant '*angulosus*' are rather similar to *A. multiformis* in that they have
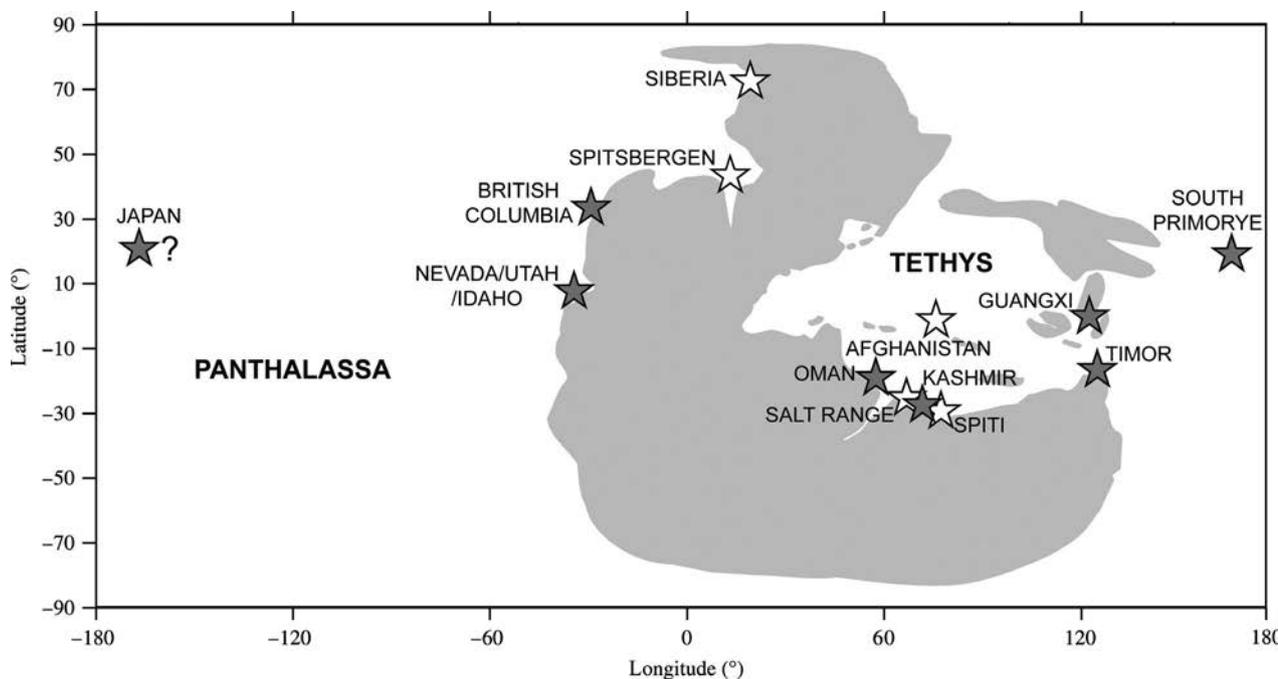
FIG. 26. Late Smithian palaeogeographical distribution of *Anasibirites kingianus* (Waagen, 1895) and *A. multiformis* Welter, 1922 (map modified from Brayard *et al.* 2009). Grey stars indicate localities where both *A. kingianus* and *A. multiformis* occur together; white stars represent localities with occurrence of *A. kingianus* only.

a subtabulate venter and thin megastriae (Fig. 17A–D). However, these rare specimens exhibit a less compressed whorl section, megastriae of highly variable magnitude on early whorls (although less conspicuous than typical *A. kingianus* specimens) and disappearance of megastriae on mature whorls, thus suggesting strong allometric growth. All of these features are typical of the species *A. kingianus.*

It is also noteworthy that extremely rare specimens of *A. multiformis* display strong ribs, especially on adult stages. This unusual ornamentation is attributed to intraspecific variation within the species and is associated with a remarkably wide whorl section and evolute coiling. Two specimens from Lower Weber Canyon (Utah) are extreme robust specimens (Figs 22B, 23C). One specimen (Fig. 23C) has strong true ribs on its inner whorls and is thus somewhat similar to the morphotype 'angulosus'. The other specimen (Fig. 22B) has extremely strong ribs on the outer whorl. Similarly, these ribs are not megastriae, but true ribs. Therefore, these two specimens do not belong to *A. kingianus*. These unusually thick and evolute specimens of *A. multiformis* are extremely rare.

A consequence of this revised taxonomy is that the *Anasibirites* fauna from Utah as reported by Brayard *et al.* (2013) apparently does not include typical representatives of *A. kingianus,* but instead probably contains only specimens attributable to *A. multiformis*. Thus, the *Anasibirites kingianus* beds should be renamed accordingly.

CONCLUSION

Extensive morphological and biometric studies indicate that the genus *Anasibirites* comprises only two valid species, namely *A. kingianus* and *A. multiformis*. In contrast to *A. kingianus*, *A. multiformis* combines a nearly isometric growth with compressed whorls and megastriae of very low magnitude at all developmental stages. *A. kingianus* also appears to be rare in Oman, whereas *A. multiformis* has not yet been recorded from the Boreal Realm (Siberia, Spitsbergen) or from the Salt Range, Spiti and Afghanistan (Fig. 26).

With regard to *A. kingianus*, most of the 'horizontal' variation (at the same developmental stage) is the direct manifestation of variability in the timing of development. This kind of intraspecific variation is classic in many Mesozoic ammonoid clades (e.g. Westermann 1966; Kennedy and Cobban 1976; Monnet *et al.* 2010). As a result of this taxonomic revision, the loss of species diversity caused by the first phase of the late Smithian extinction is significantly higher than previously estimated. The late Smithian extinction is concomitant with the inception of a global positive shift of the carbon cycle (Fig. 1; Galfetti *et al.* 2007) and a quick recovery of gymnosperms that followed the middle Smithian C-isotope negative peak and spore spike, respectively (Hermann *et al.* 2011). Abrupt changes in these climate proxies were coeval with the origination of the cosmopolitan, short-lived and

28

species-poor genus *Anasibirites* and the beginning of the late Smithian ammonoid extinction.

SYSTEMATIC PALAEONTOLOGY
by Romain Jattiot *and* Hugo Bucher

Taxonomic descriptions follow the terminology of Arkell *et al.* (1957*b*). Material described herein is reposited in the PIMUZ, Paleontological Institute and Museum of the University of Zurich, Karl Schmid-Strasse 4, 8006 Zurich, Switzerland. For details regarding the conventional abbreviations used for the synonymy lists, the reader is referred to Matthews (1973). Synonymy lists are updated based on our taxonomic revision.

Order AMMONOIDEA Zittel, 1884
Suborder CERATITINA Hyatt, 1884
Superfamily MEEKOCERATACEAE Waagen, 1895
Family PRIONITIDAE Hyatt, 1900

Genus ANASIBIRITES Mojsisovics, 1896

Type species. Sibirites kingianus Waagen, 1895; from the Salt Range, Pakistan.

Remarks. Anasibirites is herein considered to include only two valid species: *Anasibirites* (*Sibirites*) *kingianus* Waagen, 1895 (Figs 4, 6–9, 10A–M, 12, 15–18) and *Anasibirites multiformis* Welter, 1922 (Figs 10N–S, 21–23). *Anasibirites* (*Sibirites*) *angulosus* Waagen, 1895 and *Anasibirites nevolini* Zakharov, 1968 are here synonymized with *A. kingianus*.

Anasibirites kingianus (Waagen, 1895)
Figures 4, 6–9, 10A–M, 12, 15–18

  *. 1895 Sibirites kingianus Waagen, p. 108, pl. 8, figs 1–2.
  . 1895 Sibirites chidruensis Waagen, p. 109, pl. 8, figs 3–4.
  . 1895 Sibirites dichotomus Waagen, p. 111, pl. 8, figs 5–6, 9.
  . 1895 Sibirites inaequicostatus Waagen, p. 113, pl. 8, figs 7–8.
  . 1895 Sibirites ceratitoides Waagen, p. 115, pl. 8, fig. 10.
  . 1895 Sibirites discoides Waagen, p. 116, pl. 8, fig. 11.
  . 1895 Sibirites angulosus Waagen, p. 117, pl. 8, figs 12–13.
  . 1895 Sibirites parvumbilicatus Waagen, p. 119, pl. 9, figs 5–6.
  . 1895 Sibirites ibex Waagen, p. 121, pl. 9, fig. 3.
  . 1895 Sibirites hircinus Waagen, p. 123, pl. 9, fig. 4.
  ?1905 Sibirites noetlingi Hyatt and Smith, p. 49, pl. 9, figs 1–3.
  p *?1909 Sibirites spiniger* Krafft and Diener, p. 131, pl. 31, fig. 2 only.

  non. 1909 *Sibirites robustus* (=*Wasatchites*) Krafft and Diener, p. 132, pl. 31, fig. 1.
  non. 1909 *Sibirites* sp. indet. ex aff. *robusto* Krafft and Diener, p. 133, pl. 31, fig. 6.
  non. 1909 *Sibirites spitiensis* Krafft and Diener, p. 136, pl. 31, fig. 8.
  non. 1909 *Sibirites* sp. indet. Krafft and Diener, p. 138, pl. 31, figs 4–5.
  p. 1922 *Anasibirites multiformis* Welter, p. 138, pl. 15, figs 9–27; pl. 16, figs 1–10, 14, 15 only.
  . 1922 *Anasibirites robustus* Welter, p. 144, pl. 17, figs 15–17.
  . 1929 *Anasibirites kingianus* Waagen; Mathews, p. 8, pl. 7, figs 14–22.
  . 1929 *Anasibirites madisoni* Mathews, p. 11, pl. 1, figs 23–26.
  non. 1929 *Anasibirites perrini* Mathews, p. 18, pl. 3, figs 34–36.
  . 1929 *Anasibirites pseudoibex* Mathews, p. 21, pl. 3, figs 28–31; pl. 7, fig. 46.
  . 1929 *Anasibirites mcclintocki* Mathews, p. 22, pl. 4, figs 1–6.
  . 1929 *Anasibirites alternatus* Mathews, p. 23, pl. 4, figs 22–23.
  . 1929 *Anasibirites romeri* Mathews, p. 23, pl. 4, figs 24–25.
  ? 1929 *Anasibirites hyatti* Mathews, p. 30, pl. 5, figs 6–11.
  ? 1929 *Anasibirites mojsisovicsi* Mathews, p. 30, pl. 5, figs 1–3.
  ? 1929 *Gurleyites chamberlini* Mathews, p. 44, pl. 11, figs 3–5.
  ? 1929 *Gurleyites boutwelli* Mathews, p. 45, pl. 8, figs 1–3.
  ? 1929 *Gurleyites milleri* Mathews, p. 45, pl. 9, figs 10–12.
  non. 1932 *Anasibirites kingianus* var. *inaequicostatus* Waagen; Smith, p. 72, pl. 79, figs 16–17.
  . 1932 *Anasibirites multiformis* Welter; Smith, p. 74, pl. 79. fig. 18.
  ? 1932 *Anasibirites mojsisovicsi* Mathews; Smith, p. 73, pl. 80, figs 1–2.
  ? 1932 *Anasibirites noetlingi* Hyatt and Smith; Smith, p. 74, pl. 9, figs 1–3.
  . 1932 *Anasibirites tenuistriatus* Waagen; Smith, p. 74, pl. 79, figs 9–10.
  . 1932 *Anasibirites angulosus* Waagen; Smith; p. 70, pl. 79, figs 13–15.
  . 1964 *Anasibirites pacificus* Bando, p. 73, pl. 3, figs 5–7; pl. 5, figs 8, 11, 13–14; pl. 6, figs 8–9, 11.
  . 1964 *Anasibirites ehimensis* Bando, p. 74, pl. 3, figs 12a–c.
  . 1964 *Anasibirites* sp. A Bando, p. 77, pl. 3, figs 8a–c.
  p. 1968 *Anasibirites nevolini* Zakharov, p. 131, pl. 25, fig. 5 only.
  . 1968 *Anasibirites kingianus* Waagen; Kummel and Erben, p. 135, pl. 22, figs 12–17; pl. 23, figs 1–18.
  . 1978 *Anasibirites kingianus* Waagen; Guex, pl. 3, figs 2, 9; pl. 4, fig. 6.
  p. 1978 *Anasibirites nevolini* Zakharov; Zhakharov, pl. 11, figs 11–13 only.

. 1990 *Anasibirites ochotensis* Bytschkov; Dagys and Ermakova, p. 47, pl. 13, figs 2–5.

. 1994 *Anasibirites robustus* Welter; Tozer, p. 78, pl. 28, fig. 2a–b.

p ?2007 *Anasibirites kingianus* Waagen; Lucas *et al.*, p. 104, fig. 3 h–j only.

v. 2008 *Anasibirites nevolini* Zakharov; Brayard and Bucher, p. 57, pl. 28, fig. 7–9, text-fig. 49.

v p. 2012a *Anasibirites kingianus* Waagen; Brühwiler and Bucher, p. 101, figs 84E–L, 84R–U only.

v p. 2012a *Anasibirites angulosus* Waagen; Brühwiler and Bucher, p. 103, figs 84V–AA, 86A–U, 87A–D, K–M only.

v. 2012b *Anasibirites kingianus* Waagen; Brühwiler *et al.*, p. 155, figs 31O, 32AA–BD.

. 2013 *Anasibirites nevolini* Zakharov; Zakharov *et al.*, figs 6.1–6.2.

Emended diagnosis. As a general rule, early whorls evolute, quadratic, with megastriae of highly variable magnitude, thus mimicking the intercalation of stronger ribs (Fig. 5B–D). At mature stage, shell without megastriae, but with growth lines and ribs (more pronounced on the venter) on some specimens. Strong allometric growth, expressed by evolute, depressed early whorls and compressed, more involute adult whorls (Figs 11, 13, 24).

Description. This species exhibits an extremely wide intraspecific variation. Early whorls are characterized by evolute coiling, a usually quadratic but more rarely slightly compressed whorl section, and megastriae of highly variable magnitude. With further growth (>20 mm), whorl section becomes more compressed (Fig. 13) and megastriae become approximated, with a lesser magnitude. However, the diameter at which this change in sculpture and whorl section occurs is highly variable. Thus, there is a highly variable extension of robust earlier whorls (evolute coiling, quadratic whorl section and megastriae of highly variable magnitude), some specimens retaining this morphology and sculpture up to 20–25 mm (40 mm for the most extreme specimen; morphotype 'nevolini'; Fig. 12). At mature stage, the shell is fairly compressed (Fig. 13) and megastriae fade away (e.g. Fig. 7D–E). This species therefore exhibits a strong allometric growth (Fig. 24). On some specimens, ribs develop at mature stage (Fig. 9A, E). As a general rule, mature stages of *A. kingianus* are thus characterized by a shell without megastriae, with growth lines and with low rounded ribs (more pronounced on the venter) in some specimens.

Ventral shape is highly variable, ranging from tabulate with angular shoulders to arched with rounded shoulders. Juvenile stages tend to exhibit a more tabulate venter with more angular shoulders. Ventral morphology also shows an extreme ontogenetic variation. Some specimens retain a subtabulate venter with marked but rounded shoulders until the mature stage (morphotype 'angulosus'; Figs 15–17). These specimens tend to develop ribs (more pronounced on the venter) on the outer whorl (e.g. Fig. 15F; Fig. 16B, F).

The umbilicus is moderately deep with an oblique to nearly perpendicular wall and rounded umbilical shoulders. Suture line is ceratitic, with rather deep lateral lobes and broad and rounded saddles (Fig. 6B).

Occurrence. (Fig. 26) Cosmopolitan species found in Nevada, Utah and Idaho (e.g. Mathews 1929; Smith 1932), Siberia (Dagys and Ermakova 1990), Spitsbergen (Weitschat and Lehmann 1978; Piazza 2015), British Columbia (Tozer 1994), Timor (Welter 1922; this work), Spiti (Brühwiler *et al.* 2012b), Salt Range (Waagen 1895; Brühwiler *et al.* 2012c), Kashmir (RJ unpub. data), Afghanistan (Kummel and Erben 1968), Guangxi (Brayard and Bucher 2008), Oman (RJ unpub. data), South Primorye (Zakharov 1968; Zakharov *et al.* 2013) and Japan (Bando 1964).

Number of studied specimens. 903.

Anasibirites multiformis Welter, 1922
Figures 10N–S, 21–23

? 1895 *Sibirites tenuistriatus* Waagen, p. 124, pl. 9, figs 1–2.

*p. 1922 *Anasibirites multiformis* Welter, p. 138, pl. 16, figs 9–13, 16–19; pl. 17, figs 1–3, 8–10 only.

. 1927 *Ophiceras multiplicatus* Yehara, p. 162, pl. 14, figs 4, 4a.

. 1929 *Anasibirites salisburyi* Mathews, p. 9, pl. 1, figs 27–29; pl. 2, figs 1–2.

. 1929 *Anasibirites johannseni* Mathews, p. 12, pl. 1, figs 34, 36–37.

. 1929 *Anasibirites whitei* Mathews, p. 12, pl. 1, fig. 35; pl. 2, figs 15–16.

. 1929 *Anasibirites blackwelderi* Mathews, p. 13, pl. 2, figs 10–14.

. 1929 *Anasibirites fisheri* Mathews, p. 13, pl. 2, figs 3–9.

. 1929 *Anasibirites emmonsi* Mathews, p. 14, pl. 2, figs 20–26.

. 1929 *Anasibirites welleri* Mathews, p. 14, pl. 2, figs 17–19.

. 1929 *Anasibirites powelli* Mathews, p. 15, pl. 3, figs 1–5.

. 1929 *Anasibirites whitfieldi* Mathews, p. 16, pl. 3, figs 6–8.

. 1929 *Anasibirites crickmayi* Mathews, p. 16, pl. 3, figs 24–27.

. 1929 *Anasibirites veranus* Mathews, p. 17, pl. 3, figs 18–23.

. 1929 *Anasibirites perrini* Mathews, p. 18, pl. 3, figs 34–36.

. 1929 *Anasibirites ketchumi* Mathews, p. 18, pl. 3, figs 12–17.

. 1929 *Anasibirites weaveri* Mathews, p. 19, pl. 3, figs 10–11, 32–33.

. 1929 *Anasibirites wardi* Mathews, p. 19, pl. 2, figs 27–29.

. 1929 *Anasibirites clarki* Mathews, p. 25, pl. 4, figs 26–28.

. 1929 *Anasibirites bretzi* Mathews, p. 25, pl. 4, figs 14–18; pl. 7, fig. 13.

. 1929 *Anasibirites vanbuskirki* Mathews, p. 26, pl. 4, figs 36–38.

. 1929 *Anasibirites rollini* Mathews, p. 27, pl. 1, figs 30–33; pl. 4, figs 10–13.

. 1929 *Anasibirites gibsoni* Mathews, p. 29, pl. 5, figs 4–5.

. 1932 *Anasibirites hircinus* Waagen; Smith, p. 72, pl. 79, figs 11–12.

. 1932 *Anasibirites emmonsi* Mathews; Smith, p. 71, pl. 79, figs 22–24.

? 1932 *Anasibirites desertorum* Smith, p. 71, pl. 51, figs 7–10; pl. 56, figs 19–20.

. 1964 *Anasibirites onoi* Bando, p. 72, pl. 3, figs 13a–b, 14a–b, 15a–d, 16; pl. 5, fig. 7.

? 1964 *Anasibirites intermedius*; Bando, p. 75, pl. 5, figs 9a–b.

. 1964 *Anasibirites multiplicatus* Yehara; Bando, p. 76, pl. 3, figs 4a–b, 9a–b, 11a–b, 13a–b, 17; pl. 5, figs 10, 15.

?1964 *Anasibirites* sp. B Bando, p. 77, pl. 3, figs 1–2.

?1964 *Anasibirites* sp. C Bando, p. 78, pl. 5, fig. 12.

p. 1978 *Anasibirites nevolini* Zhakarov, pl. 11, figs 9–10 only.

. 1981 *Meekoceras* sp. Dean, pl. 1, fig. 5.

. 1994 *Anasibirites crickmayi* Mathews; Tozer, p. 78, pl. 28, fig. 1a–b.

. 2007 *Anasibirites kingianus* Waagen; Lucas *et al.*, p. 104, figs 3d–g; figs 4a–b, e–h, j–l.

v. 2008 *Anasibirites multiformis* Welter; Brayard and Bucher, p. 56, pl. 28, figs 1–6, text-figs 48–49.

. 2010 *Anasibirites kingianus* Waagen; Stephen *et al.*, fig. 7a–b.

v. 2012b *Anasibirites multiformis* Welter; Brühwiler and Bucher, p. 33, pl. 19, figs 1–6.

p. 2013 *Anasibirites kingianus* Waagen; Brayard *et al.*, p. 195, fig. 62a–g, j-k only.

. 2013 *Anasibirites multiformis* Welter; Brayard *et al.*, p. 195, fig. 64a–g.

. 2013 *Anasibirites simanenkoi* Zakharov *et al.*, p. 603, figs 6.3–6.8.

Description. This species exhibits nearly isometric growth (Figs 11, 24) and a moderately involute shell. Venter is tabulate to subtabulate, with angular shoulders on inner whorls and subtabulate with bluntly angular shoulders on mature whorls. Umbilicus is relatively shallow with an oblique wall and rounded shoulders. Flanks are subparallel and flat on inner whorls. Sculpture typically consists of dense megastriae of very low magnitude (Fig. 5A) throughout ontogeny (even on mature whorls). Suture line is ceratitic with rather deep lateral lobes and broad and rounded saddles (Fig. 21H).

Occurrence. (Fig. 26) Cosmopolitan species found in Nevada, Utah and Idaho (e.g. Brayard *et al.* 2013), British Columbia (Tozer 1994), Timor (Welter 1922; this work), Salt Range? (Waagen 1895), Kashmir (RJ unpub. data), Guangxi (Brayard

and Bucher 2008), Oman (Brühwiler *et al.* 2012a), South Primorye (Zakharov *et al.* 2013) and Japan (Bando 1964).

Number of studied specimens. 52.

REFERENCES

ARKELL, W. J., KUMMEL, B. and WRIGHT, C. W. 1957a. Mesozoic Ammonoidea. 80–465. *In* MOORE, R. C. (ed.). *Treatise on invertebrate paleontology, Part L, Mollusca 4: Cephalopoda, Ammonoidea.* Geological Society of America, Boulder, CO & University of Kansas Press, Lawrence, KS, 490 pp.

—— FURNISH, W. M., KUMMEL, B., MILLER, A. K., MOORE, R. C., SCHINDEWOLF, O. H., SYLVESTER-BRADLEY, P. C. and WRIGHT, C. W. 1957b. Cephalopoda, Ammonoidea. 1–490. *In* MOORE, R. C. (ed.). *Treatise on invertebrate paleontology, Part L, Mollusca 4.* Geological Society of America, Boulder, CO & University of Kansas Press, Lawrence, KS, 490 pp.

BANDO, Y. 1964. The Triassic stratigraphy and ammonite fauna of Japan. *The Science Reports of the Tohoku University, Sendai, Japan – Second Series (Geology)*, **36**, 1–137.

BRAYARD, A. and BUCHER, H. 2008. Smithian (Early Triassic) ammonoid faunas from northwestern Guangxi (South China): taxonomy and biochronology. *Fossils & Strata*, **55**, 1–179.

—— BRÜHWILER, T., BUCHER, H. and JENKS, J. 2009. Guodunites, a low-palaeolatitude and trans-Panthalassic Smithian (Early Triassic) ammonoid genus. *Palaeontology*, **52**, 471–481.

—— BYLUND, K. G., JENKS, J. F., STEPHEN, D. A., OLIVIER, N., ESCARGUEL, G., FARA, E. and VENNIN, E. 2013. Smithian ammonoid faunas from Utah: implications for Early Triassic biostratigraphy, correlation and

basinal paleogeography. *Swiss Journal of Palaeontology*, **132** (2), 141–219.

BRÜHWILER, T. and BUCHER, H. 2012*a*. Systematic palaeontology. 22–111. *In* BRÜHWILER, T., BUCHER, H., WARE, D., HERMANN, E., HOCHULI, P. A., ROOHI, G., REHMAN, K. and YASSEN, A. (eds) *Smithian (Early Triassic) ammonoids from the Salt Range*. Special Papers in Palaeontology, **88**, 1–114.

—— —— 2012*b*. Systematic palaeontology. 13–107. *In* BRÜHWILER, T., BUCHER, H., GOUDEMAND, N. and GALFETTI, T. (eds) *Smithian (Early Triassic) ammonoids faunas from exotic blocks from Oman: taxonomy and biochronology*. Palaeontographica, Abteilung A, **296**, 3–107.

—— —— BRAYARD, A. and GOUDEMAND, N. 2010. High-resolution biochronology and diversity dynamics of the Early Triassic ammonoid recovery: the Smithian faunas of the Northern Indian Margin. *Palaeogeography, Palaeoclimatology, Palaeoecology*, **297** (2), 491–501.

—— —— ROOHI, G., YASEEN, A. and REHMAN, K. 2011. A new early Smithian ammonoid fauna from the Salt Range (Pakistan). *Swiss Journal of Palaeontology*, **130** (2), 187–201.

—— —— GOUDEMAND, N. and GALFETTI, T. 2012*a*. Smithian (Early Triassic) ammonoids faunas from exotic blocks from Oman: taxonomy and biochronology. *Palaeontographica, Abteilung A*, **296**, 3–107.

—— —— and KRYSTYN L. 2012*b*. Middle and late Smithian (Early Triassic) ammonoids from Spiti, India. *Special Papers in Palaeontology*, **88**, 115–174.

—— —— WARE, D., HERMANN, E., HOCHULI, P. A., ROOHI, G., REHMAN, K. and YASSEN, A. 2012*c*. Smithian (Early Triassic) ammonoids from the Salt Range. *Special Papers in Palaeontology*, **88**, 1–114.

BUCHER, H. and GUEX, J. 1990. Rythmes de croissance chez les ammonites triasiques. *Bulletin de la Société vaudoise des sciences naturelles*, **80** (2), 191–209.

—— LANDMAN, N. H., KLOFAK, S. M. and GUEX, J. 1996. Mode and rate of growth in ammonoids. 407–461. *In* LANDMAN, N. H. (ed.). *Ammonoid paleobiology*. Plenum Press, New York, 857 pp.

BURGESS, S. D., BOWRING, S. and SHEN, S,-Z. 2014. High-precision timeline for Earth's most severe extinction. *Proceedings of the National Academy of Sciences*, **111** (9), 3316–3321.

CHARLTON, T. R., BARBER, A. J., MCGOWAN, A. J., NICOLL, R. S., RONIEWICZ, E., COOK, S. E., BARKHAM, S. T. and BIRD, P. R. 2009. The Triassic of Timor: Lithostratigraphy, chronostratigraphy and palaeogeography. *Journal of Asian Earth Sciences*, **36**, 341–363.

DAGYS, A. S. and ERMAKOVA, S. P. 1990. *Early Olenekian ammonoids of Siberia*. Nauka, Moscow, 112 pp.

DAVIS, J. C. 2002. *Statistics and data analysis in geology*. Third edition. John Wiley & Sons, 646 pp.

DE BAETS, K., BERT, D., HOFFMANN, R., MONNET, C., YACOBUCCI, M. M. and KLUG, C. 2015. Ammonoid intraspecific variability. 359–426. *In* KLUG, C., KORN, D., DE BAETS, K., KRUTA, I. and MAPES, R. H. (eds). *Ammonoid paleobiology: from anatomy to ecology*. Topics in Geobiology, **43**, Springer, 937 pp.

DEAN, J. S. 1981. Carbonate petrology and depositional environments of the Sinbad Limestone Member of the Moenkopi Formation in the Teasdale Dome Area, Wayne and Garfield Counties, Utah. *Brigham Young University Geology Studies*, **28**, 19–51.

DIENER, C. 1895. Himalayan fossils—the Cephalopoda of the Muschelkalk. *Palaeontologia Indica*, Series 15, II, **2**, 1–118.

GALFETTI, T., BUCHER, H., OVTCHAROVA, M., SCHALTEGGER, U., BRAYARD, A., BRÜHWILER, T., GOUDEMAND, N., WEISSERT, H., HOCHULI, P. A., CORDEY, F. and GUODUN, K. 2007. Timing of the Early Triassic carbon cycle perturbations inferred from new U-Pb ages and ammonoid biochronozones. *Earth & Planetary Science Letters*, **258** (3), 593–604.

GUEX, J. 1978. Le Trias inférieur des Salt Ranges (Pakistan): problèmes biochronologiques. *Eclogae Geologicae Helvetiae*, **71**, 105–141.

HAMMER, Ø. and HARPER, P. B. 2006. *Paleontological data analysis*. Blackwell Publishing, 351 pp.

HERMANN, E., HOCHULI, P. A., BUCHER, H., BRÜHWILER, T., HAUTMANN, M., WARE, D. and ROOHI, G. 2011. Terrestrial ecosystems on North Gondwana in the aftermath of the end-Permian mass extinction. *Gondwana Research*, **20** (2), 630–637.

HYATT, A. 1884. Genera of fossil cephalopods. *Proceedings of the Boston Society of Natural History*, **22**, 253–338.

—— 1900. Cephalopoda. 502–604. *In* ZITTEL, K. A. V. and EASTMAN, C. R. (eds). *Textbook of paleontology*. Macmillan & Co., London, 706 pp.

—— and SMITH, J. 1905. The Triassic cephalopod genera of America. *US Geological Survey Professional Paper*, **40**, 1–394.

KENNEDY, W. J. and COBBAN, W. A. 1976. Aspects of ammonite biology, biogeography, and biostratigraphy. *Special Papers in Palaeontology*, **17**, 1–94.

KOMATSU, T., SHIGETA, Y., HUYEN, D. T., TIEN, D. C., MAEKAWA, T. and TANAKA, G. 2013. *Crittendenia* (Bivalvia) from the Lower Triassic (Olenekian) Bac Thuy Formation, An Chau Basin, Northern Vietnam. *Paleontological Research*, **17** (1), 1–11.

KRAFFT, A. V. and DIENER, C. 1909. Lower Triassic Cephalopoda from Spiti, Malla Johar, and Byans. *Palaeontologia Indica*, **6**, 1–186.

KRUMBECK, L. 1924. Die Brachiopoden, Lamellibranchiaten und Gastropoden der Trias von Timor II. Paläontologischer Teil. 1–142. *In* WANNER, J. (ed.). *Paläontologie von Timor, Volume 22*. E. Schweizerbart'sche Verlagsbuchhandlung (Erwin Nägele), Stuttgart, 275 pp.

KUMMEL, B. and ERBEN, H. K. 1968. Lower and Middle Triassic cephalopods from Afghanistan. *Palaeontographica*, **129**, 95–148.

LUCAS, S. G., GOODSPEED, T. H. and ESTEP, J. W. 2007. Ammonoid biostratigraphy of the Lower Triassic Sinbad Formation, East-Central Utah. *New Mexico Museum of Natural History and Science Bulletin*, **40**, 103–108.

MAEDA, H. 1993. Dimorphism of Late Cretaceous false-puzosiine ammonites, *Yokoyamaoceras* Wright and Matsumoto,

1954 and *Neopuzosia* Matsumoto, 1954. *Transactions and Proceedings of the Palaeontological Society of Japan, New Series*, **169**, 97–128.

MARTINI, R., ZANINETTI, L., VILLENEUVE, M., CORNÉE, J.-J., KRYSTYN, L., CIRILLI, S., DE WEVER, P., DUMITRICA, P. and HARSOLUMAKSO, A. 2000. Triassic pelagic deposits of Timor: palaeogeographic and sea-level implications. *Palaeogeography, Palaeoclimatology, Palaeoecology*, **160** (1), 123–151.

MATHEWS, A. A. L. 1929. The Lower Triassic cephalopod fauna of the Fort Douglas area, Utah. *Walker Museum Memoirs*, **1**, 1–46.

MATSUMOTO, T. 1991. The mid-Cretaceous ammonites of the family Kossmaticeratidae from Japan. *Palaeontological Society of Japan, Special Papers*, **33**, 1–143.

—— MURAMOTO, T. and INOMA, A. 1972. Two small desmoceratid ammonites from Hokkaido. *Transactions and Proceedings of the Palaeontological Society of Japan, New Series*, **87**, 377–394.

MATTHEWS, S. C. 1973. Notes on open nomenclature and synonymy lists. *Palaeontology*, **16**, 713–719.

MOJSISOVICS, E. V. 1886. Arktische Triasfaunen. *Mémoires de l'Académie Impériale des sciences de Saint Petersbourg, VIIe série*, **33**, 1–159.

—— 1896. Beitrage zur Kenntnis der obertriadischen Cephalopoden-Faunen des Himalaya. *Denkschriften der Akademie der Wissenschaften in Wien*, **63**, 573–701.

MONNET, C., BUCHER, H., WASMER, M. and GUEX, J. 2010. Revision of the genus *Acrochordiceras* Hyatt, 1877 (Ammonoidea, Middle Triassic): morphology, biometry, biostratigraphy and intra-specific variability. *Palaeontology*, **53** (5), 961–996.

—— DE BAETS, K. and YACOBUCCI, M. M. 2015. Buckman's rules of covariation. 67–94. *In* KLUG, C., KORN, D., DE BAETS, K., KRUTA, I. and MAPES, R. H. (eds). *Ammonoid paleobiology: from macroevolution to paleogeography.* Topics in Geobiology, **44**, Springer, 600 pp.

NEWELL, N. D. and BOYD, D. W. 1995. Pectinoid bivalves of the Permian-Triassic crisis: *American Museum of Natural History. Bulletin*, **227**, 1–95.

OBATA, I., FUTAKAMI, M., KAWASHITA, Y. and TAKAHASHI, T. 1978. Apertural features in some Cretaceous ammonites from Hokkaido, *Bulletin of the National Science Museum. Series C (Geology)*, **4** (3), 139–155.

OVTCHAROVA, M., BUCHER, H., SCHALTEGGER, U., GALFETTI, T., BRAYARD, A. and GUEX, J. 2006. New Early to Middle Triassic U-Pb ages from South China: calibration with ammonoid biochronozones and implications for the timing of the Triassic biotic recovery. *Earth & Planetary Science Letters*, **243** (3), 463–475.

—— GOUDEMAND, N., HAMMER, Ø., GUODUN, K., CORDEY, F., GALFETTI, T., SCHALTEGGER, U. and BUCHER, H. 2015. Developing a strategy for accurate definition of a geological boundary through radio-isotopic and biochronological dating: the Early-Middle Triassic boundary (South China). *Earth-Science Reviews*, **146**, 65–76.

PIAZZA, V. 2015. Late Smithian (Early Triassic) ammonoids from the uppermost Lusitaniadalen Member (Vikinghøgda

Formation), Svalbard. Msc Thesis, University of Oslo, 135 pp.

POMPECKJ, J. F. 1884. Über Ammonoideen mit anomaler Wohnkammer. *Jahresbericht des Vereins für vaterländische Naturkunde in Württemberg*, **49**, 220–290.

R CORE TEAM. 2014. *R: A language and environment for statistical computing*. R Foundation for Statistical Computing, Vienna, Austria. http://www.r-project.org/.

REYMENT, R. A. and SAVAZZI, E. 1999. *Aspects of multivariate statistical analysis in geology*. Elsevier, 285 pp.

SMITH, J. P. 1932. Lower Triassic ammonoids of North America. *US Geological Survey Professional Paper*, **167**, 1–199.

STEPHEN, D. A., BYLUND, K. G., BYBEE, P. J. and REAM, W. J. 2010. Ammonoid beds in the Lower Triassic Thaynes Formation of western Utah, USA. 243–252. *In* TANABE K., SHIGETA, Y., SASAKI, T. and HIRANO, H. (eds) *Cephalopods—present and past.* Tokai University Press, Tokyo.

TEISSEYRE, L. 1889. Über die systematische Bedeutung der sog. Parabeln der Perisphincten. *Neues Jahrbuch für Mineralogie, Geologie und Paläontologie, Beilage-Bände*, **6** (1), 570–643.

TOZER, E. T. 1982. Marine Triassic faunas of North America: their significance for assessing plate and terrane movement. *Geologische Rundschau*, **71** (3), 1077–1104.

—— 1991. Relationship between spines, parabolic nodes, rhythmic shell secretion and formation of septa in some Triassic ammonoids. 23–24. *In The Ammonoidea: evolution and environmental change.* Systematics Association, Symposium, London, Programme Abstracts.

—— 1994. Canadian Triassic ammonoid faunas. *Geologic Survey of Canada Bulletin*, **467**, 1–663.

—— and CALON, T. J. 1990. Triassic ammonoids from Jabal Safra and Wadi Alwa, Oman, and their significance. *Geological Society, London, Special Publications*, **49**, 203–211.

URDY, S., GOUDEMAND, N., BUCHER, H. and CHIRAT, R. 2010. Allometries and the morphogenesis of the molluscan shell: a quantitative and theoretical model. *Journal of Experimental Zoology Part B: Molecular and Developmental Evolution*, **314** (4), 280–302.

WAAGEN, W. 1895. Salt Range fossils. Vol 2: Fossils from the Ceratite Formation. *Palaeontologia Indica*, **13**, 1–323.

WÄHNER, F. 1894. Beitrage zur Kenntniss der tieferen Zonen des unteren Lias in der nordöstliche Alpen. *Beiträge zur Paläontologie Österreich-Ungarns und des Orients*, **9** (1–2), 1–54.

WANNER, J. 1913. Geologie von Westtimor. *Geologische Rundschau*, **4** (2), 136–150.

WEITSCHAT, W. and LEHMANN, U. 1978. Biostratigraphy of the uppermost part of the Smithian stage (Lower Triassic) at the Botneheia, W-Spitsbergen. *Mitteilungen aus dem Geologischen, Paläontologisches Institut, Universität Hamburg*, **48**, 85–100.

WELTER, O. A. 1922. Die ammoniten der Unteren Trias von Timor. *Paläontologie von Timor*, **11** (2).

WESTERMANN, G. E. G. 1966. Covariation and taxonomy of the Jurassic ammonite *Sonninia adicra* (Waagen). *Neues Jahrbuch für Geologie und Paläontologie Abhandlungen*, **124**, 289–312.

YEHARA, S. 1927. The Lower Triassic cephalopod and bivalve fauna of Shikoku. *Japanese Journal of Geology and Geography*, **5** (4), 135–172.

ZAKHAROV, Y. D. 1968. *Lower Triassic biostratigraphy and ammonoids of South Primorye*. Nauka, Moscow, 175 pp. [in Russian]

—— 1978. *Lower Triassic ammonoids of East USSR*. Nauka, Moscow, 224 pp. [in Russian]

—— BONDARENKO, L. G., SMYSHLYAEVA, O. P. and POPOV, A. M. 2013. Late Smithian (Early Triassic) ammonoids from the *Anasibirites nevolini* Zone of South Primorye, Russian Far East. *New Mexico Museum of Natural History and Science*, **61**, 597–612.

ZITTEL, K. A. V. 1884. *Handbuch der Paläontologie. Mollusca und Arthropoda*. R. Oldenbourg, Munich, 839 pp.